Anthropogenic contributions to atmospheric Hg, Pb and As accumulation recorded by peat cores from southern Greenland and Denmark dated using the ^{14}C "bomb pulse curve"

W. Shotyk,[1,*] M. E. Goodsite,[2,†] F. Roos-Barraclough,[3,‡] R. Frei,[4] J. Heinemeier,[5] G. Asmund,[6] C. Lohse,[7] and T. S. Hansen[7]

[1]Institute of Environmental Geochemistry, University of Heidelberg, INF 236, D-69120 Heidelberg, Germany
[2]Department of Atmospheric Environment, National Environmental Research Institute of Denmark, Frederiksborgvej 399, P.O. Box 358, DK-4000 Roskilde, Denmark
[3]Institute of Geological Sciences, University of Berne, Baltzerstrasse 1-3, CH-3012 Berne, Switzerland
[4]Geological Institute, University of Copenhagen, Øster Voldgade 10, DK-1350 Copenhagen, Denmark
[5]AMS 14C Dating Laboratory, IFA, Aarhus University, Aarhus, Denmark
[6]Department of Arctic Environment, National Environmental Research Institute, Frederiksborgvej 399, P.O. Box 358, DK-4000 Roskilde, Denmark
[7]Environmental Chemistry Research Group, Department of Chemistry, University of Southern Denmark, Odense University, Campusvej 55, Odense M, Denmark

Abstract—Mercury concentrations are clearly elevated in the surface and sub-surface layers of peat cores collected from a minerotrophic ("groundwater-fed") fen in southern Greenland (GL) and an ombrotrophic ("rainwater-fed") bog in Denmark (DK). Using ^{14}C to precisely date samples since ca. AD 1950 using the "atmospheric bomb pulse," the chronology of Hg accumulation in GL is remarkably similar to the bog in DK where Hg was supplied only by atmospheric deposition: this suggests not only that Hg has been supplied to the surface layers of the minerotrophic core (GL) primarily by atmospheric inputs, but also that the peat cores have preserved a consistent record of the changing rates of atmospheric Hg accumulation. The lowest Hg fluxes in the GL core (0.3 to 0.5 μg/m^2/yr) were found in peats dating from AD 550 to AD 975, compared to the maximum of 164 μg/m^2/yr in AD 1953. Atmospheric Hg accumulation rates have since declined, with the value for 1995 (14 μg/m^2/yr) comparable to the value for 1995 obtained by published studies of atmospheric transport modelling (12 μg/m^2/yr).

The greatest rates of atmospheric Hg accumulation in the DK core are also found in the sample dating from AD 1953 and are comparable in magnitude (184 μg/m^2/yr) to the GL core; again, the fluxes have since gone into strong decline. The accumulation rates recorded by the peat core for AD 1994 (14 μg/m^2/yr) are also comparable to the value for 1995 obtained by atmospheric transport modelling (18 μg/m^2/yr). Comparing the Pb/Ti and As/Ti ratios of the DK samples with the corresponding crustal ratios (or "natural background values" for preanthropogenic peat) shows that the samples dating from 1953 also contain the maximum concentration of "excess" Pb and As. The synchroneity of the enrichments of all three elements (Hg, Pb, and As) suggests a common source, with coal-burning the most likely candidate. Independent support for this interpretation was obtained from the Pb isotope data (^{206}Pb/^{207}Pb = 1.1481 ± 0.0002 in the leached fraction and 1.1505 ± 0.0002 in the residual fraction) which is too radiogenic to be explained in terms of gasoline lead alone, but compares well with values for U.K. coals. In contrast, the lowest values for ^{206}Pb/^{207}Pb in the DK profile (1.1370 ± 0.0003 in the leached fraction and 1.1408 ± 0.0003 in the residual fraction) are found in the sample dating from AD 1979: this shows that the maximum contribution of leaded gasoline occurred approximately 25 yr *after* the zenith in total anthropogenic Pb deposition. *Copyright © 2003 Elsevier Ltd*

1. INTRODUCTION

Atmospheric pollution in the industrial regions of the northern hemisphere is increasingly recognised as a potential threat to many life forms in the Arctic (AMAP, 1998). The present state of the Arctic environment has been summarised as follows (Braune et al., 1999): 1) some native groups are among the most exposed populations in the world to certain environmental pollutants; 2) the levels of organic and inorganic contaminants in birds and mammals may exceed thresholds associated with reproductive, immunosuppressive, and neurobehavioral effects; 3) mercury seems to be increasing in aquatic sediments and in marine mammals, and tends to accumulate in marine food webs. The most significant knowledge gap at the present time is the "lack of temporal trend information for most contaminants" (Braune et al., 1999).

In contrast to the other "heavy metals" of environmental concern, Hg can be singled out as a truly global pollutant because 1) more than 95% of atmospheric Hg is in the vapour phase where it has a residence time of at least one year (Lin and Pehkonen, 1999) and can be transported thousands of kilometres (Schroeder and Munthe, 1998), and 2) it is the only metal which indisputably biomagnifies through the food chain, as inorganic forms of the metal are methylated by bacteria (Lindberg et al., 1987). Accumulation of Hg in the Arctic environ-

ment is of particular concern because of bioaccumulation of its methylated forms (Morel et al., 1998) and their potential toxicity (Fitzgerald and Clarkson, 1991). However, the relative importance of natural versus anthropogenic sources of Hg to the Arctic is poorly understood and there is an urgent need for long term records to quantify fluxes due to anthropogenic emissions.

To quantify the effects of human activities of the atmospheric geochemical cycle of Hg, the natural variability in the Hg cycle must be known, and this can only be obtained using long-term records of Hg accumulation. Ombrotrophic peat bogs receive inputs exclusively from the air (Clymo, 1987). Boyarkina et al. (1980) suggested that peat cores from these types of bogs preserve a record of the changing rates of atmospheric Hg deposition. This view has been supported by independent experimental evidence (Oechsle, 1982), and by several subsequent studies of Hg concentrations in dated peat cores from temperate bogs (Pheiffer-Madsen, 1981; Jensen and Jensen, 1991; Norton et al., 1997; Benoit et al., 1998; Biester et al., 2002; Bindler, 2003). The first long-term reconstruction of atmospheric Hg deposition was obtained using a Spanish bog which has been accumulating peat since since 4070 ^{14}C yr BP; this study not only showed that anthropogenic sources have exceeded natural contributions for more than a millenium (Martinez-Cortizas et al., 1999), but also that cold climate phases promote atmospheric Hg accumulation which has important implications for polar regions. More recently, a peat bog in Switzerland (Etang de la Gruère in the Jura Mountains) has been used to create a high-resolution reconstruction of atmospheric Hg deposition extending back 14500 calendar years (Roos-Barraclough et al., 2002a): here, the natural range of Hg fluxes (0.3 to 8 $\mu g/m^2/yr$) was found to be impacted both by Holocene climate change and volcanic emissions. Anthropogenic Hg was quantified using the natural range of Hg to Br to calculate "excess" Hg; this revealed the appearance of anthropogenic Hg beginning in the late Medieval Period. A subsequent study of a neighbouring peat bog in the Swiss Jura provided a comparable chronology of atmospheric Hg accumulation, even though the second bog (La Tourbière des Genevez) became predominately minerotrophic with increasing depth (Roos-Barraclough and Shotyk, 2003). Thus, the chemical weathering reactions which have been taking place in the basal sediment underlying the peat bog had not contributed significantly to the Hg inventory of the profile. The maximum rates of atmospheric Hg accumulation in the Swiss peat bog profiles was 29–43 $\mu g/m^2/yr$, with higher rates consistently found in the forested bog (TGE).

To date, there are no long term records of atmospheric Hg deposition for the Arctic, and the relative importance of natural versus anthropogenic sources to such remote areas has aroused controversy (Rasmussen, 1994; Fitzgerald et al., 1997). To address this problem, we measured Hg concentration profiles in mires from Greenland and Denmark which have been accumulating peat for more than 3000 yr (Goodsite, 2000). In fact, the south Greenland site is sub-Arctic but the core collected here is of special importance because the past 50 yr of peat accumulation has been precisely dated with ^{14}C using the "atmospheric bomb pulse" (Goodsite et al., 2002); this offers the promise of a detailed reconstruction of recent changes. As the peat profile from Denmark was also age dated using the same, high preci-

sion approach (Goodsite et al., 2002), it was also included in our study for comparison.

To compare with Hg, we have also studied Pb which is transported primarily in the fine (submicron) aerosol fraction (Puxbaum, 1991). Several characteristics of Pb render this element a particularly useful tracer for studying atmospheric deposition of trace metals and organic contaminants. First, it is known to be well preserved in ombrotrophic bogs (Vile et al., 1995, 1999; Shotyk et al., 1996, 1997; MacKenzie et al., 1997, 1998; Weiss et al., 1999a,b), with bogs recording Pb chronologies which are comparable with lake sediment archives (Brännvall et al., 1997; Martinez-Cortizas et al., 1997; Farmer et al., 1997; Norton et al., 1997) and historical records of ancient Pb mining (Kempter et al., 1997; Kempter and Frenzel, 1999, 2000). Second, long-term changes in the environmental pollution record of this element in Europe is comparatively well established (e.g., Shotyk et al., 1998, 2001, 2003). Third, Pb has a number of radiogenic isotopes which can be used to "fingerprint" the predominant sources of atmospheric pollutants (Kober et al., 1999; Bollhöfer and Rosman, 2001; Flament et al., 2002; Reuer and Weiss, 2002). Finally, we also measured As as this element is commonly enriched in coal (Bouska, 1981; Valkovic, 1983; Swaine, 1990).

2. MATERIAL AND METHODS

2.1. Description of the Peat Deposits

The two peatlands studied are distinctly different with respect to hydrology, geochemistry and trophic status: an acidic (pH 4) ombrotrophic bog in Denmark contrasts strongly with a circumneutral (pH 7) minerotrophic fen in Greenland.

The peatland near the village of Tasiusaq in southern Greenland (GL) is a small, confined subarctic fen on the Narsaq peninusla (61° 08.314′ N, 45° 33.703′ W) of southern Greenland (Fig. 1). The average annual temperature and rainfall at Narsarsuaq airport (opposite the fjord) were 0.9 °C and 615 mm, respectively, from 1961 to 1990 (Danish Meteorological Institute, Technical Report 00-18). The site was cored in September 1999, towards the end of the growing season. Representative plant species and photos of the fen as well as the general area are given elsewhere (Goodsite, 2000). The maximum thickness of peat accumulation is ca. 1 m. The basal material is predominately clay, with aquatic plant species dominating the deepest 10 cm of peat accumulation (W.O. van der Knaap, University of Berne, personal communication); ascending from this zone, the peat consists predominately of mosses. The fen developed between two small lakes, and may have formed through the terrestrialization of a shallow lake basin. A small brook, ca. 1m wide and 1 m deep, runs through the fen, connecting the lakes. Topographically the mire is in a valley between steep mountains - but there was no visual indication that the peat deposit may have formed from a landslide. The fen surface today is characterized by small hummocks (20 to 40 cm high), and the ground is very spongy.

The bedrock geology of this part of S. Greenland belongs to the Qassiarsuk complex which consists of a sequence of alkaline silicate tuffs and extrusive carbonatites interlayered with sandstones and their subvolcanic equivalents (Andersen, 1997). This complex is located in a roughly E-W trending graben structure between the village of Qassiarsuk and the settlement of Tasiusaq in the northern part of the Precambrian Gardar rift. Uranium mineralisations corresponding to the alkaline igneous activities have been found, with the alkaline, high conductivity waters marked by anomalous U concentrations both in the aqueous phases and in the sediments (Armour-Brown et al., 1983).

Storelung Mose in Denmark is a typical raised *Sphagnum* bog (55° 15.38′ N, 10°15.37′ E) on the Island of Funen (Fig. 1). The average annual temperature and rainfall were 8.1 °C and 639 mm, respectively, from 1961 to 1990 (Danish Meteorological Institute, Technical Report 99–5). The bog had a history of peat digging lasting through the end of
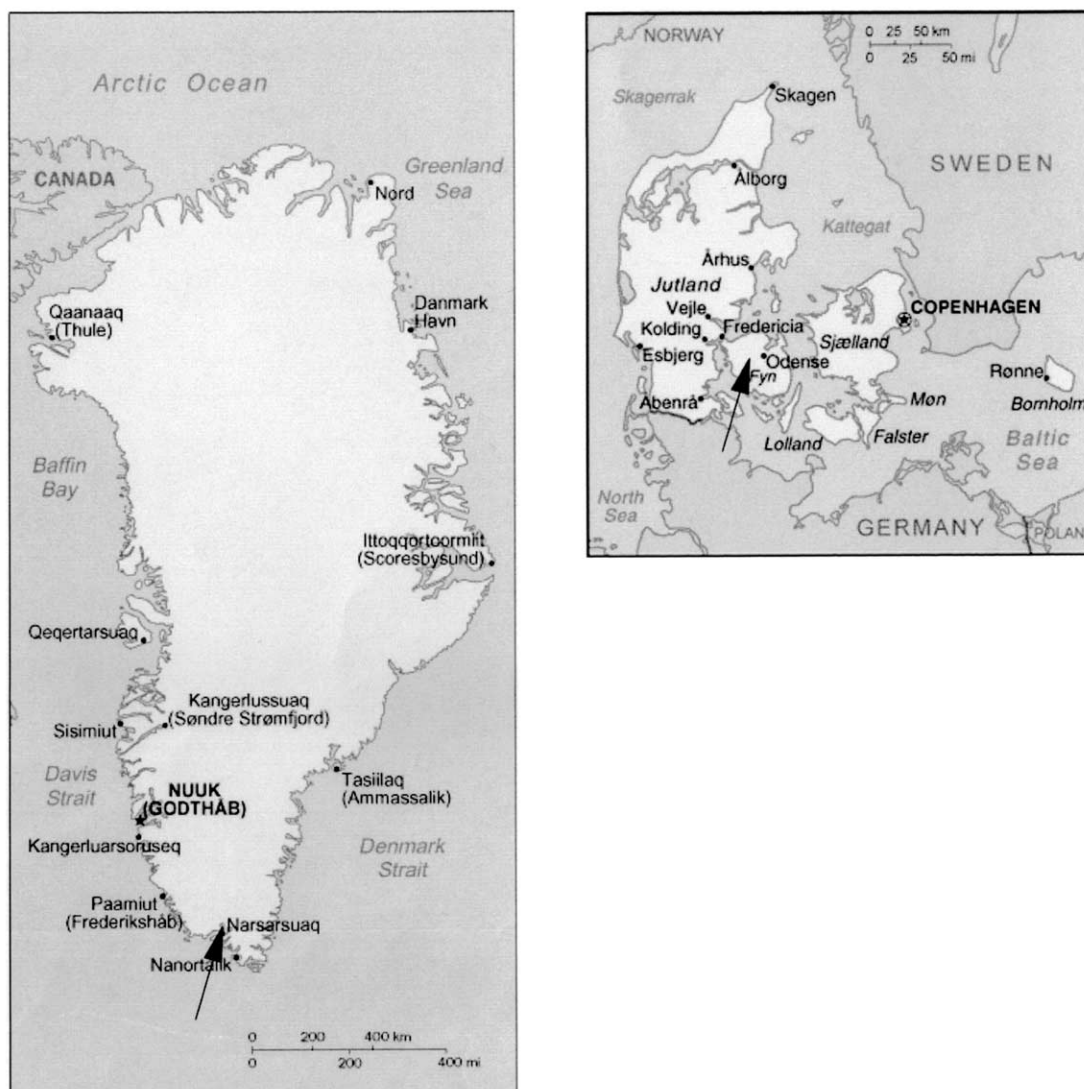
Fig. 1. Location maps of the coring sites in Greenland (GL) and Denmark (DK).

WWII (Bent Aaby, Danish National Museum, personal communication): this fact had been established before core collection, but the condition was considered tolerable as this study emphasises the chronology of atmospheric Hg, Pb, and As deposition since AD 1950 (which is datable using the ^{14}C atmospheric bomb pulse procedure). With most of the peat bogs in Denmark having been destroyed by man, the number of remaining possible coring sites which are suitable for atmospheric deposition studies really is rather limited. The bog is situated in a rural farming community, and when viewed from the edge, is seen to rise above the landscape. The peat deposit is 5 to 6 m deep with a relatively flat microtopography (Asbirk et al., 1973). Today's bog bears visible scars of disturbance, with an overgrown cart road through the middle of the bog, and excavation pits close to the trail. The pits are now overgrown with mats of moss. The sampling site chosen was as far from visible signs of peat digging as possible, in the NE section of the bog. Samples were collected in October, 1999 from zones intermediate in relief between hummocks and hollows.

2.2. Sample Collection and Preparation

Coring sites were located with obvious peat accumulation and three (15 cm × 15 cm by approximately 100 cm) monoliths of peat were cored at each site using a Ti Wardenaar peat sampler (Wardenaar, 1987). Three cores (labelled A, B, and C) were taken at each site, with each ca. 1.5 m apart, and forming a triangle. "A" cores were cut into 3 cm slices by hand in the field, and porewaters were expressed by hand for subsequent chemical analyses.

2.3. Chemical Analyses of Porewaters and the Trophic Status of the Mires

Pore water samples were kept cool. Upon returning to the lab, all water samples were filtered to exclude material greater than 0.2 μm using polysulfone membrane filters (Acrodisc, Gelman), and refrigerated. Anions (Cl^- and Br^-) and cations (Na^+, K^+, Mg^{2+}, Ca^{2+}) in the waters were measured using chemically suppressed ion chromatography with conductivity detection (Steinmann and Shotyk, 1997). Each of the porewater samples was analyzed in duplicate both for anions and for cations.

The pH of the surface waters at GL is neutral to alkaline and the porewaters typically contain ca. 20 mg/L Ca^{2+}; this is typical of minerotrophic fens and indicates the importance of mineral dissolution reactions, both within the peatland and in the surrounding basin, which control the composition of the waters (Shotyk, 1988). In contrast to the

GL fen, the pH of the bog waters from DK is acidic (pH 4) and the porewaters contain only ca. 2 mg/L Ca^{2+}; this is typical of ombrotrophic bogs, and shows that mineral dissolution reactions are quantitatively insignificant: this is true because of the limited supply of minerals for reaction with the surface waters of the bog. The low pH value and low concentrations of Ca^{2+} in the porewaters, therefore, indicates that mineral matter is supplied to the DK core only from the atmosphere, and this must be true also of trace metals such as Hg and Pb.

2.4. Measurement of Pb and Other Trace Element Analyses Using XRF

Peat cores were frozen within one day of sample collection, and shipped frozen to the lab in Berne. Individual slices from the "A" cores were partially thawed and a Plexiglas template (10×10 cm) was used to allow the outer 2.5 cm of each slice to be trimmed away using an acid rinsed ceramic knife on a plastic cutting board; clean lab procedures were followed, cleaning the cutting board and knife with deionized water three times between each slice. The edges cut off the slices were dried overnight at 105 °C in a drying oven and milled in a centrifugal mill equipped with a Ti rotor and 0.25 mm Ti sieve (Ultracentrifugal Mill ZM 1-T, F. K. Retsch GmbH and Co., Haan, Germany). The milled powder from pieces of each slice was then manually homogenized before using the powder for further analysis. Selected major and trace elements (K, Ca, Ti, Cr, Mn, Fe, Ni, Cu, Zn, As, Br, Rb, Sr, Y, Zr and Pb) were measured using the Energydispersive Miniprobe Multielement Analyzer (EMMA) using Mo $K\beta$ as the exciting radiation. The lower limits of detection for the elements reported here, on a dry weight basis, are Mn 12, Fe 5, Cu 1, As 3.0, Se 0.4, Br 0.7, Rb 0.5, Sr 0.6, Y 1.0, Zr 1.5, Pb 0.4 and U 2 $\mu g/g$. Calibration of the instrument using international, certified, standard reference materials (SRMs), and the accuracy and precision of the trace metal measurements, are described in detail elsewhere (Cheburkin and Shotyk, 1996; Shotyk et al., 2000). Using the EMMA XRF, As concentrations are calculated as $([Pb]+[As]) - [As]$ but this is acceptable considering the abundance of As in the surface layers of the DK core (see below). Moreover, As is used here only to compare its distribution with that of Hg and Pb.

The XRF data from the 3 cm slices (core A) not only provides quantitative information about the concentrations of various elements in the peat profiles, but also offers a general indication of the trophic status of the sites.

Ash contents were measured by combustion at 550 °C overnight.

2.5. Measurement of Hg

The second set of cores (GL and DK "B" cores) were used for Hg analyses and age dating. One cm slices were cut while frozen using a stainless steel band saw. The "zero" depth of the monolith was taken to represent the interface between the living plant material at the top, and the underlying dead plant matter (peat); this transition was typically 3 cm below the top of the core. Individual slices were subsampled using a stainless steel microcorer (ca. 16 mm ID) to recover ca. 2 cm^3 plugs from every cm down to 40 cm, and every 2nd cm below 40 cm; these were air-dried overnight at room temperature in a class 100 laminar flow clean air cabinet. Mercury concentrations were measured in these plugs using solid sample atomic absorption spectroscopy (Salvato and Pirola, 1996) with a LECO AMA 254 as described in detail elsewhere (Roos-Barraclough et al., 2002b). The instrument was calibrated using liquid Hg working standards prepared from a Merck 1000 mg/L Hg standard solution. Every 12th measurement was a certified reference material, either NIST 1515 (Apple Leaves) or NIST 1547 (Peach Leaves). The average measured values were 45.0 ± 0.7 ng/g (n=11) for NIST 1515 (certified value 44 ± 4 ng/g) and 32.1 ± 1.4 ng/g (n=15) for NIST 1547 (certified value 31 ± 7 ng/g). The Hg concentration profiles presented here (analyst: F. R-B.) are in excellent agreement with those reported previously (analyst: M.E.G.) for selected samples from the same cores (Goodsite, 2000).

As an independent check on the data which are presented here, Hg concentrations were also measured in a complete set of subsamples at the Department of Arctic Environment, Danish National Environmental Research Institute (analyst: G.A.). Approximately 1 g fresh sample and 4 mL concentrated Merck Suprapur nitric acid were added to

Teflon bombs with stainless steel caps, which were then heated for 12 h at 150°C. After cooling the dissolved samples were left uncovered until the majority of the nitrous oxides had evaporated. Before analysing for Hg, potassium permanganate solution was added until a permanent pink colour was obtained to maintain an oxidising environment and to prevent loss of Hg. The samples were then diluted with 18 mol/LΩ water to approximately 25 g in polyethylene bottles. Mercury concentrations were determined following reduction with sodium borohydride in a flow injection AAS system (Perkin Elmer FIMS). The data set obtained using this procedure is in good agreement with the data which is presented in this paper, obtained using the LECO AMA 254 (on average, within 15%, $r^2 = 0.727$, n=65).

2.6. Age Dating Using ^{14}C

Plant macrofossils identified in selected samples from each "B" core were ^{14}C dated by using Accelerator Mass Spectrometry (AMS). The macrofossils were taken from the centers of selected one-cm slices at the Institute of Plant Science, University of Berne, where they were also cleaned and dried at 60 °C. Within one week of selection they were processed at the AMS ^{14}C Dating Laboratory, University of Aarhus, using a standard procedure for plant material (washed, acid-base-acid treatment). Individual samples more recent than AD 1950 were dated directly by comparing the measured ^{14}C concentrations in the samples with the atmospheric concentrations of ^{14}C recorded since the beginning of thermonuclear bomb testing; these tests greatly increased the amount of ^{14}C in the atmosphere, resulting in an "atmospheric bomb pulse" (ABP). The high resolution age dates obtained this way are ± 2 yr. All details describing the AMS ^{14}C dating method and the application of the atmospheric bomb pulse, as well as a comparison with ^{210}Pb age dating of the same set of peat samples, is given elsewhere (Goodsite et al., 2002). Since the publication of that paper (Goodsite et al., 2002), approximately twice the number of samples has been age dated, with all results summarised here (Tables 1, 2). Selected samples from deeper layers (before AD 1950) were AMS ^{14}C dated by the usual tree-ring calibration method; here, the uncertainties are much greater (Tables 1, 2).

In addition to the ^{14}C age dates obtained using AMS, the basal peat sample from each "A" core was dated using ^{14}C decay counting (Physics Institute, University of Berne) which yielded ages of 3540 ± 30 and 2790 ± 40 ^{14}C yr BP for the bottom sample of the GL (78cm) and DK (84cm) cores, respectively.

2.7. Stable Pb Isotopes

Powdered samples of peat were analysed at the Danish Center for Isotope Geology for stable lead isotopes (^{204}Pb, ^{206}Pb, ^{207}Pb, ^{208}Pb) in two fractions: weak acid leachates which are designed to recover predominantly atmospheric lead adhering to the plant material, and from the corresponding residues which primarily represents geogenic lead hosted in the inorganic, minerotrophic matrix, as well as atmospherically-derived soil dust (Table 3). Leaching of the peat material was performed with 2N HCl for two hours. The samples were then centrifuged and the supernatant was carefully pipetted off. The residues were attacked by 8N HBr for 1 d, then dried and subsequently re-attacked using an HF-HNO_3 mixture for 2 d in Savillex Teflon beakers. This procedure has been shown to be effective in dissolving both phosphates and silicates (Frei et al., 1997; Schaller et al., 1997). Lead was processed and separated over 0.5 mL glass columns charged with a 100 mesh AG-1 x8 anion exchange resin (BIORAD) and purified in a second clean-up over 200 μl Teflon columns containing the same resin. Liquid aliquots of both leachates and residues were doped with a ^{204}Pb spike for isotope dilution concentration measurements. Lead separates were loaded with a 1M H_3PO_4 - silica-gel mix and measured from 20 μm Re-filaments on a VG-54 Sector-IT thermal ionization mass spectrometer at the Geological Institute, University of Copenhagen. Lead isotopes were analyzed in static multi-collection mode. Procedural blanks remained below 110 pg Pb: this is insignificant relative to the amount of Pb contained in the samples. Isotopic fractionation of Pb was monitored by repeated analyses of the NBS-SRM 981 Pb standard, and the measured data were corrected for mass bias using the values of Todt et al. (1993).

Table 1. AMS ^{14}C dating of plant macrofossils from the peat core (GL2B) from Tasiusaq, Greenland.

Lab nr AAR-	Average depth (cm)	δ^{13}C (‰)	Conv. ^{14}C age (BP)	^{14}C content (pMC)	Calibrated age[1]
5620	0.5	−26.2	−840 ± 40	110.99 ± 0.57	1957;**1996–1999**
5621	0.0	−28.3	−900 ± 45	111.88 ± 0.62	1957;**1994–1999**
5622	−0.5	−26.8	−1075 ± 40	114.34 ± 0.57	1957–1958;**1991–1994**
6861	−1.5	−26.55	−1180 ± 40	115.84 ± 0.58	1958;**1989–1992**
6899	−2.5	−26.62	−1090 ± 30	114.54 ± 0.41	1957–1958;**1991–1993**
6862	−3.5	−26.05	−2150 ± 35	130.65 ± 0.54	1962;**1978–1979**
5623	−5.5	−26.3	−2720 ± 35	140.33 ± 0.61	1962;**1973–1974**
5624	−7.5	−25.8	−2880 ± 40	143.13 ± 0.69	1962;**1973**
5625	−9.5	−25.9	−3890 ± 35	162.32 ± 0.72	1963;**1967**
5626	−12.5	−27.6	−4685 ± 35	179.13 ± 0.83	**1963–1965**
5627	−14.5	−26.7	−1895 ± 35	126.62 ± 0.59	**1961–1962**;1980–1981
5628	−16.5	−27.2	−1535 ± 35	121.07 ± 0.54	**1958–1961**
5629	−18.5	−27.1	−200 ± 40	102.52 ± 0.54	**1956**
6900	−26.5	−24.59	65 ± 40	99.18 ± 0.51	AD: 1700–1720; 1810–1830; 1880–1920; 1950–55
6901	−29.5	−25.29	130 ± 40	98.38 ± 0.52	AD: 1670–1760; 1800–1890; 1910–1950
6620	−36.5	−33.3	1095 ± 45	87.24 ± 0.51	AD: 890–1000
6621	−54.5	−23.6	1115 ± 45	87.04 ± 0.50	AD: 890–985
6622	−74.5	−26.6	2485 ± 45	73.39 ± 0.41	BC: 770–520
6623	−80.5	−26.6	2845 ± 50	70.19 ± 0.42	BC: 1110–1100; 1080-920
5630	−87.5	−26.7	2920 ± 50	69.52 ± 0.44	BC: 1210–1010

[1]) Calibrated age ranges corresponding to 95% confidence interval for depths 0–18.5 cm, and 68% confidence interval for depths 26.5–87.5 cm.

3. RESULTS

3.1. Mercury Concentrations in Relation to Ash Contents and Dry Bulk Density

The large differences in ash contents illustrate the fundamental hydrological differences between the two peat profiles. In the GL core (Fig. 2a), ash concentrations are in the range of ca. 10 to 40% whereas the peat samples below 30 cm in the DK core typically contain ca. 2% ash (Fig. 2b); these values are typical of minerotrophic and ombrotrophic peats, respectively (Naucke et al., 1993). There is an exceptional zone of elevated ash content in the DK core at ca. 18cm (Fig. 2b) which may reflect the disturbance of the bog surface by peat cutting during WWII. Bulk density values are generally higher in the GL core (Fig. 2a) compared to DK core (Fig. 2b).

The Hg concentration profiles reveal elevated Hg concentrations in both the upper and lower sections of the GL core (Fig. 2b), but only in the upper section of the DK core (Fig. 2b). To take into account the large differences in bulk density within and between the two cores, the Hg concentrations are also expressed on a volumetric basis (Fig. 2). The variation in volumetric Hg concentrations above 30 cm show a remarkable similarity between the two cores, with a very intense peak in volumetric Hg concentration in the GL core at 21 cm (Fig. 2a) and in the DK core at 17 cm (Fig. 2b), respectively. The selected age dates shown in Figure 2 indicate that the zone of greatest Hg concentration in each core dates from the 1950's. The very old radiocarbon ages in the DK peat samples below 29 cm (which was dated at 2395 ± 45 ^{14}C yr BP) is evidence that some part of the original peat surface has been lost due to peat cutting. These old sections of the DK profile will not be considered further.

3.2. Mercury Concentrations in Ombrotrophic (DK) versus Minerotrophic (GL) Peat Profiles

The chronology of changes in volumetric Hg concentrations is remarkably similar at the two sites (Fig. 2). The DK core is ombrotrophic, therefore Hg was supplied to this profile exclusively by atmospheric deposition. The greatest Hg concentrations are found in samples dating from the 1950's. As there are no known natural geochemical processes which could have led to this pronounced Hg enrichment, we assume that the elevated Hg concentrations in the surface layers, compared to deeper, older peats, reflect increased rates of atmospheric Hg deposition caused by industrial activities. Similarly, in the GL core the greatest Hg concentrations are found in samples dating from the 1950's. In contrast to the DK core, the GL profile is minerotrophic, and the possible importance of Hg provided by mineral-water reactions has to be carefully considered. However, we know of no natural geochemical processes which could have enriched the surface of this core with Hg without also enriching the middle section of the core, between ca. 30 and 55 cm, which contain the lowest Hg concentrations. We further assume, therefore, that the elevated Hg concentrations in the surface layers of the GL core also can be attributed to atmospheric Hg inputs. Other possible causes of the changes in Hg concentrations in the GL core will be discussed later in the paper.

3.3. Atmospheric Hg Accumulation Rates in Southern Greenland

The age dates given in Table 1 can be used to calculate an age-depth model to estimate peat accumulation rates (Fig. 3). This process identifies three regions, indicated by the three

Table 2. AMS ^{14}C dating of plant macrofossils from the peat core (DK1B) from Storelung Mose, Denmark.

Lab nr AAR-	Average depth (cm)	δ^{13}C (‰)	Conv ^{14}C age (yrs BP)	^{14}C content (pMC)	Calibrated age[1]
5611	0.0	−27.5	−865 ± 40	111.36 ± 0.54	1957;**1995–1999**
5612	−0.5	−26.1	−860 ± 45	111.31 ± 0.61	1957;**1995–1999**
5613	−2.5	−26.8	−1180 ± 45	115.84 ± 0.65	1958; **1989–1992**
6855	−3.5	−26.88	−1830 ± 35	125.62 ± 0.53	1961; **1980–1982**
6856	−4.5	−26.25	−2210 ± 40	131.65 ± 0.65	1962; **1978–1979**
6857	−5.5	−24.92	−2520 ± 45	136.88 ± 0.75	1962; **1975–1976**
6858	−6.5	−23.93	−2785 ± 40	141.44 ± 0.70	1962; **1973–1974**
6859	−7.5	−23.24	−3465 ± 35	153.92 ± 0.69	1963; **1970–1971**
5614	−8.5	−24.3	−3400 ± 40	152.68 ± 0.76	1963; **1970**
6860	−9.5	−22.78	−4580 ± 30	176.82 ± 0.68	**1963–1965**
6612	−10.5	−23.0	−2529 ± 43	136.99 ± 0.74	**1962;** 1975–1976
6613	−11.5	−24.0	−1707 ± 42	123.68 ± 0.65	**1959–1961;** 1982–1984
6614	−12.5	−23.6	−1926 ± 42	127.09 ± 0.67	**1962;** 1980–1981
6615	−13.5	−24.3	−746 ± 47	109.74 ± 0.65	**1957;** 1995–1999
5615	−14.5	−24.7	−1480 ± 35	120.19 ± 0.55	**1958;** 1960; 1984–1987
5616	−15.5	−25.7	−1505 ± 35	120.58 ± 0.56	**1958–1961;** 1984–1987
5617	−16.5	−27.0	−10 ± 45	100.12 ± 0.53	AD: 1693–1726; 1813–1850; 1862–1918; **1951–1956**
5618	−18.5	−24.2	45 ± 40	99.43 ± 0.49	AD: 1895–1905; 1951–55
6898	−19.5	−25.34	160 ± 40	98.00 ± 0.49	AD: 1660–1700; 1720–1820; 1850–1870; 1910–1950
6616–1	−28.5	−26.7	2395 ± 45	74.20 ± 0.43	BC: 760-720; 540-390
6616–2	−28.5	−27.5	380 ± 45	95.41 ± 0.55	AD: 1440–1520; 1590–1630
6617–1	−34.5	−25	3225 ± 50	66.94 ± 0.42	BC: 1600–1590; 1530–1430
6617–2	−34.5	−28.7	2720 ± 45	71.29 ± 0.41	BC: 905–820
6618	−46.5	−26.7	2935 ± 50	69.40 ± 0.43	BC: 1260–1240; 1220–1040
6619	−68.5	−26.5	2970 ± 50	69.11 ± 0.45	BC: 1300–1080; 1060–1050
5619	−78.5	−24.5	3050 ± 45	68.39 ± 0.38	BC: 1390–1260; 1230–1220

[1]) Calibrated age ranges corresponding to 95% confidence interval for depths 0–16.5 cm, and 68% confidence interval for depths 18.5–78.5 cm.

regression lines (Fig. 3). These regression lines serve as an age model from which the age of any depth can be deduced. In the ca. 3000 yr period before AD 1950, the average peat accumulation rate was 0.019 cm/yr (Fig. 3a); from AD 1950 to ca. 1976, the accumulation rate was 0.68 cm/yr, and since ca. 1976, the rate has been 0.20 cm/yr (Fig. 3b). The age depth model allows the atmospheric Hg accumulation rate to be estimated as the product of the volumetric Hg concentrations (ng/cm3) and the peat accumulation rate (cm/yr). Strictly speaking, the atmospheric Hg accumulation rate calculated in this way is equal to the depositional flux minus re-emission of Hg from the peatland surface. Experimental studies using peat (Lodenius et al., 1983) have shown that Hg re-emissions are small (i.e., <0.01% of total Hg added as ^{203}Hg) so that the atmospheric Hg accumulation rates shown here (in units of μg/m^2/yr versus age in Fig. 4) are comparable to the depositional fluxes. These results show that the net, preindustrial Hg accumulation rate ranged from 0.3 to 3 μg/m^2/yr (Fig. 4a) which is comparable to the range (0.3 to 8 μg/m^2/yr) obtained from ca. 12500 BC to 1300 AD using a Swiss peat bog profile (Roos-Barraclough et al., 2002a). The graph shows further that the net Hg accumulation rate before AD 200 was in the range 1 to 3 μg/m^2/yr, whereas samples from AD 550 to AD 975 were in the range 0.3 to 0.5 μg/m^2/yr (Fig. 4a). While some part of this variation in preindustrial accumulation rates may be due to Holocene cli-

mate change (Martinez-Cortizas et al., 1999; Roos-Barraclough et al., 2002a), the elevated Hg concentrations in samples below 55 cm (dated at AD 938 ± 48 (Fig. 2b) are found in minerotrophic peats, and we cannot yet separate the Hg concentrations into atmospheric, aquatic, and terrestrial components. However, it is clear that the preindustrial, net rates of Hg accumulation in GL were in the range 0.3 to 3 μg/m^2/yr (Fig. 4a), placing an upper limit on the natural atmospheric Hg flux.

In contrast to the "natural background" Hg accumulation rate, the flux in GL reached 164 μg/m^2/yr in 1953 (Fig. 4b). The value in 1995 (14.1 μg/m^2/yr) is an order of magnitude lower, but still exceeds by a wide margin the natural range in net Hg accumulation rate shown in Figure 4b. The value obtained here for 1995 is in good agreement with the Danish Eulerian Hemisphere model calculations (12.0 μg/m^2/yr in 1995) published for South Greenland (Christensen et al., 2002), supporting the approach used here to estimate the atmospheric Hg fluxes. The error associated with the Hg fluxes (Fig. 4) is calculated to be 21%, based on conservative estimates of the errors associated with the ^{14}C bomb pulse curve age dates (ca. 5%), Hg concentrations (ca. 5%), and bulk density measurements (ca. 20%). Even after the upper and lower limits on the flux data are added to Figure 4, the temporal trends in net atmospheric Hg accumulation rates are clear.

Table 3. Pb isotope data of leachates and residues from DK and GL peatlands

Sample	Depth	Phase	Acid*	Time	Pb (ppm)	206Pb/204Pb	± 2s+	207Pb/204Pb	± 2s+
DK 1B 0+, L, IC		0 leachate	2N HCl	1h	8.28	17.872	0.092	15.508	0.081
DK 1B 1–2, L, IC		2 leachate	2N HCl	1h	24.24	17.726	0.025	15.562	0.023
DK 1B 4–5, L, IC		5 leachate	2N HCl	1h	32.48	17.683	0.021	15.553	0.020
DK 1B 7–8, L, IC		8 leachate	2N HCl	1h	49.91	17.762	0.024	15.548	0.022
DK 1B 12–13, L, IC		13 leachate	2N HCl	1h	113.79	17.910	0.021	15.561	0.019
DK 1B 15–16, L, IC		16 leachate	2N HCl	1h	141.41	17.866	0.022	15.562	0.020
DK 1B 18–19, L, IC		19 leachate	2N HCl	1h	84.08	17.928	0.021	15.557	0.019
DK 1B 30–31, L, IC		31 leachate	2N HCl	1h	2.38	18.396	0.053	15.608	0.046
DK 1B 40–41, L, IC		41 leachate	2N HCl	1h	16.55	18.365	0.025	15.600	0.022
DK 1B 48–49, L, IC		49 leachate	2N HCl	1h	14.38	18.112	0.039	15.436	0.034
DK 1B 78–79, L, IC		79 leachate	2N HCl	1h		17.639	0.063	15.128	0.055
DK 1B 0+, R, IC		0 residue	8N HBr-HF	1d	1.27	17.241	0.168	14.892	0.146
DK 1B 1–2, R, IC		2 residue	8N HBr-HF	1h	10.19	17.787	0.022	15.560	0.022
DK 1B 4–5, R, IC		5 residue	8N HBr-HF	1h	6.02	17.744	0.019	15.554	0.018
DK 1B 7–8, R, IC		8 residue	8N HBr-HF	1h	14.32	17.795	0.016	15.555	0.015
DK 1B 12–13, R, IC		13 residue	8N HBr-HF	1h	28.8	17.937	0.033	15.566	0.029
DK 1B 15–16, R, IC		16 residue	8N HBr-HF	1d	32.08	17.897	0.012	15.556	0.013
DK 1B 18–19, R, IC		19 residue	8N HBr-HF	1d	15.33	17.979	0.024	15.570	0.022
DK 1B 30–31, R, IC		31 residue	8N HBr-HF	1d	1.15	18.361	0.035	15.588	0.031
DK 1B 40–41, R, IC		41 residue	8N HBr-HF	1d	5	18.396	0.037	15.602	0.033
DK 1B 48–49, R, IC		49 residue	8N HBr-HF	1d	2.01	18.043	0.098	15.333	0.083
DK 1B 78–79, R, IC		79 residue	8N HBr-HF	1d		18.023	0.066	15.464	0.057
GL 2B 0+, L, IC		0 leachate	2N HCl	1h	1.57	18.603	0.072	15.266	0.060
GL 2B 5–6, L, IC		5 leachate	2N HCl	1h	1.63	19.510	0.041	15.644	0.034
GL 2B 14–15, L, IC		15 leachate	2N HCl	1h	6.1	18.593	0.092	15.520	0.077
GL 2B 16–17, L, IC		17 leachate	2N HCl	1h	7.54	18.556	0.064	15.517	0.054
GL 2B 20–21, L, IC		21 leachate	2N HCl	1h	5.47	20.073	0.023	15.714	0.019
GL 2B 26–27, L, IC		27 leachate	2N HCl	1h	3.2	20.142	0.051	15.705	0.041
GL 2B 30–31, L, IC		31 leachate	2N HCl	1h	2.93	19.380	0.023	15.442	0.019
GL 2B 88+, L, IC		88 leachate	2N HCl	1h	7.08	19.417	0.037	15.347	0.030
GL 2B 0+, R, IC		0 residue	8N HBr-HF	1d	1.25	18.816	0.088	14.992	0.071
GL 2B 5–6, R, IC		5 residue	8N HBr-HF	1d	1.63	19.510	0.041	15.644	0.034
GL 2B 14–15, R, IC		15 residue	8N HBr-HF	1d	1.45	19.053	0.121	15.208	0.097
GL 2B 16–17, R, IC		17 residue	8N HBr-HF	1d	3.08	18.846	0.068	15.428	0.056
GL 2B 20–21, R, IC		21 residue	8N HBr-HF	1d	5.66	19.388	0.059	15.565	0.048
GL 2B 26–27, R, IC		27 residue	8N HBr-HF	1h	3.24	20.594	0.068	15.653	0.052
GL 2B 30–31, R, IC		31 residue	8N HBr-HF	1d	1.76	19.611	0.058	15.228	0.046
GL 2B 88+, R, IC		88 residue	8N HBr-HF	1d	5.01	20.038	0.051	15.419	0.040
UGS 1878-P, L, IC		leachate	2N HCl	1h	74.88	17.821	0.025	15.583	0.023
UGS 1878-P, R, IC		residue	8N HBr-HF	1d	7.21	17.684	0.071	15.489	0.063
GL 2B 5–6, L, IC		5 leachate	2N HCl	1h	4.45	19.158	0.053	15.508	0.044

208Pb/204Pb	± 2s+	206Pb/207Pb	± 2s+	208Pb/206Pb	± 2s+	208Pb/207Pb	r1**	r2††
37.549	0.196	1.1525	0.0006	2.1010	0.0012	2.4213	0.992	0.994
37.528	0.057	1.1390	0.0003	2.1172	0.0008	2.4116	0.979	0.968
37.485	0.050	1.1370	0.0003	2.1198	0.0008	2.4102	0.969	0.961
37.566	0.055	1.1424	0.0002	2.1149	0.0008	2.4161	0.980	0.970
37.725	0.049	1.1509	0.0002	2.1063	0.0008	2.4243	0.976	0.961
37.714	0.051	1.1481	0.0002	2.1109	0.0008	2.4235	0.978	0.962
37.773	0.049	1.1524	0.0002	2.1070	0.0008	2.4280	0.974	0.958

Table 3. continued

Sample	Depth	Phase	Acid*	Time	Pb (ppm)	206Pb/204Pb	± 2s+	207Pb/204Pb ± 2s+
38.285	0.113	1.1786	0.0004	2.0812	0.0009	2.4529	0.990	0.989
38.288	0.056	1.1773	0.0003	2.0848	0.0008	2.4544	0.977	0.968
37.823	0.084	1.1734	0.0003	2.0883	0.0010	2.4504	0.986	0.978
36.952	0.135	1.1660	0.0004	2.0949	0.0009	2.4427	0.993	0.993
36.125	0.354	1.1577	0.0008	2.0953	0.0019	2.4257	0.996	0.996
37.566	0.053	1.1432	0.0005	2.1120	0.0011	2.4143	0.923	0.935
37.530	0.046	1.1408	0.0002	2.1151	0.0008	2.4129	0.977	0.958
37.596	0.040	1.1440	0.0002	2.1128	0.0008	2.4171	0.968	0.946
37.781	0.073	1.1523	0.0003	2.1063	0.0009	2.4272	0.979	0.976
37.732	0.036	1.1505	0.0002	2.1083	0.0010	2.4255	0.947	0.886
37.868	0.055	1.1547	0.0003	2.1063	0.0008	2.4321	0.975	0.970
38.184	0.077	1.1779	0.0003	2.0796	0.0010	2.4497	0.982	0.972
38.311	0.081	1.1791	0.0003	2.0826	0.0009	2.4556	0.986	0.980
37.638	0.205	1.1768	0.0004	2.0860	0.0010	2.4548	0.996	0.996
37.743	0.140	1.1655	0.0005	2.0942	0.0011	2.4407	0.988	0.991
37.592	0.148	1.2186	0.0005	2.0208	0.0013	2.4625	0.986	0.986
38.815	0.086	1.2472	0.0004	1.9895	0.0010	2.4812	0.971	0.972
38.001	0.189	1.1980	0.0004	2.0438	0.0011	2.4486	0.995	0.994
37.981	0.133	1.1958	0.0004	2.0468	0.0010	2.4477	0.990	0.990
39.070	0.050	1.2774	0.0002	1.9464	0.0007	2.4863	0.973	0.961
39.296	0.107	1.2825	0.0004	1.9509	0.0016	2.5021	0.976	0.952
40.932	0.053	1.2550	0.0002	2.1122	0.0008	2.6508	0.974	0.962
38.297	0.076	1.2652	0.0003	1.9724	0.0008	2.4955	0.982	0.979
36.424	0.173	1.2550	0.0005	1.9358	0.0011	2.4295	0.991	0.992
38.815	0.086	1.2472	0.0004	1.9895	0.0010	2.4812	0.971	0.972
36.777	0.235	1.2528	0.0006	1.9303	0.0012	2.4183	0.992	0.995
37.591	0.138	1.2215	0.0004	1.9946	0.0010	2.4365	0.990	0.990
37.105	0.115	1.2456	0.0004	1.9138	0.0009	2.3838	0.989	0.989
37.497	0.126	1.3157	0.0003	1.8207	0.0010	2.3956	0.992	0.988
37.269	0.114	1.2877	0.0004	1.9005	0.0011	2.4473	0.985	0.983
39.894	0.105	1.2996	0.0004	1.9909	0.0011	2.5873	0.976	0.979
37.647	0.059	1.1436	0.0003	2.1126	0.0011	2.4159	0.972	0.947
37.412	0.155	1.1417	0.0006	2.1156	0.0016	2.4154	0.988	0.982
37.339	0.107	1.2354	0.0004	1.9490	0.0010	2.4078	0.983	0.982

Fig. 2. a) Ash contents (%), dry bulk density (g/cm^3), gravimetric (ng/g) and volumetric (ng/cm^3) Hg concentrations in the GL "B" cores (cut into 1 cm slices). b) Ash contents (%), dry bulk density (g/cm^3), gravimetric (ng/cm^3) and volumetric (ng/cm3) Hg concentrations in the DK "B" cores. Selected age dates (from Tables 1 and 2) are shown for convenience.

3.4. Atmospheric Hg Accumulation Rates in Southern Denmark

While the DK core cannot be used to model the age-depth relationship for samples older than WWII, the age dates (Table 2) yield an average peat accumulation rate from AD 1950 to AD 1980 of 0.47 cm/yr, and since AD 1980 of 0.21 cm/yr (Fig. 3d). Using these peat accumulation rates, the net atmospheric Hg accumulation rate can be calculated and is shown in Figure 4c. This graph shows that the maximum net Hg accumulation rate was 184 μg/m^2/yr in AD 1953 and that the flux has since gone into a strong decline. The value obtained from this peat core for 1994 (14 μg/m^2/yr) is comparable to the Danish Eulerian Hemisphere model calculations (18 μg/m^2/yr in 1995) published for Denmark (Christensen et al., 2002).

The elevated ash content in the DK core which reaches a maximum at 15–16 cm (Fig. 2b), is probably a consequence of disturbance to the peat profile; unfortunately, this layer is adjacent to the zone of maximum Hg concentration at 16–17 cm (Fig. 2b). It is difficult to determine what effect this disturbance may have had on the Hg concentration profile, the peat growth rate and therefore the Hg accumulation rate. However, the maximum Hg accumulation rates presented here (Fig. 4) are comparable to those published using other Danish peat cores by Pheiffer-Madsen (1981). In addition, Hg and Br concentrations were measured in a peat core which we collected in the spring of 2000 from Store Vildmose, a second ombrotrophic bog in

Denmark. In the Store Vildmose core, the "background" Hg/Br ratio is 0.32 × 10^{-3} ± 0.12 × 10^{-3} (average of 41 samples below 20 cm) and the maximum Hg/Br ratio (3.05 ×10^{-3}) found from 6 to 7 cm exceeds this value by 9.6 times (data not shown). In the Storelung Mose profile described in this paper, the maximum Hg/Br ratio (3.73 ×10^{-3}) exceeds this background ratio by 11.7 times. Thus, the changes in Hg/Br at Storelung Mose, despite the disturbance by peat cutting in the past, are comparable in magnitude to the changes recorded by the peat core collected from Store Vildmose (Shotyk, unpublished data). In addition, the maximum Hg concentration in the Store Vildmose core (348 ng/g) and the maximum in Hg/Br (3.05 ×10^{-3}) were dated to AD 1953 using ^{210}Pb; this agrees remarkably well with the age date of the peak in Hg concentration at Storelung (AD 1953) which was determined using the bomb pulse curve of ^{14}C (Fig. 2b). In summary, the Hg concentration data presented here for the Storelung bog, as well as the Hg/Br ratios and the chronology of Hg accumulation, are comparable to our unpublished data for these parameters from the Store Vildmose bog.

3.5. Comparison of Pb and As Concentrations and Enrichments, GL versus DK

Lead and As concentrations are much higher in the DK core compared with GL (Fig. 5a). However, the maximum Pb concentrations in the DK core are very similar to the maximum
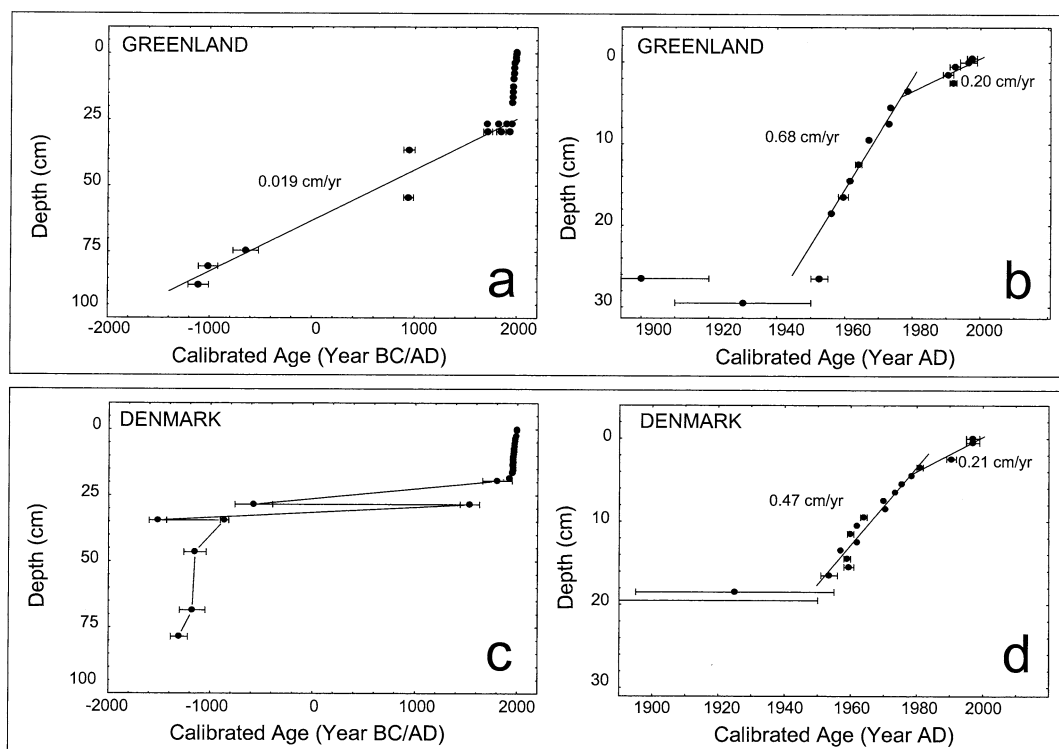
Fig. 3. Age depth relationship in the GL "B" core. a) all samples. b) samples dated using the bomb pulse curve for [14]C. Age depth relationship in the DK "B" core. a) all samples. b) samples dated using the bomb pulse curve for [14]C.

values found in the Draved Mose peat profile described by Aaby and Jacobsen (1978). To emphasize the difference in Pb and As between the GL and DK profiles, and to take into account the differences in abundance of mineral material, Enrichment Factors (EF) were calculated as

$$EF = ([M]/[Ti])_{peat}/([M]/[Ti])_{Earth's\ crust} \qquad (i)$$

where [M] refers to the total concentration of Pb or As measured in the peat sample (μg/g) and [Ti] to the total concentration of Ti. Although Sc is the preferred reference element for these calculations (Shotyk et al., 2001), Sc concentration data is not yet available for these two peat cores. The EF indicates the extent of elemental enrichment in the peats, relative to the abundance of that metal in the Earth's Upper Crust (Wedepohl, 1995) where Pb = 14.8, As = 1.7 and Ti = 4010 μg/g. The calculated Enrichment Factors (Fig. 5a) show that these elements are enriched in the DK core up to 65× (Pb) and 85× (As). In contrast, the GL core reveals no significant enrichment of Pb, and only very slight enrichments of As. Given that the As concentrations in the GL profile are generally at or below the lower limit of detection by XRF (3 μg/g), any record of anthropogenic As in the GL profile cannot be discerned using the total concentrations of As as measured by XRF, and its ratio to Ti. Similarly, in the GL core the Pb concentrations are comparatively low and concentrations of lithogenic trace elements such as Ti and Zr are comparatively high; thus, using total metal concentrations it is not possible to discern any significant impact of anthropogenic Pb. In the DK core, just the opposite is true: concentrations of Pb and As are high but the

concentrations of lithogenic elements (Ti, Zr) are comparatively low. Thus, in the DK core, enrichments of Pb and As, relative to their crustal abundance, are clearly seen (Fig. 5a).

3.6. Changing Atmospheric Pb Fluxes in Denmark

In the DK core, all of the Pb was derived from the atmosphere. Given the immobility of Pb in ombrotrophic peat bog profiles (Shotyk et al., 1997, 1998, 2001, 2002b; Weiss et al., 1999a,b and references cited therein), the atmospheric Pb flux can be calculated (Fig. 5b) using the average peat accumulation rates, the Pb concentrations, and the bulk density data. This flux can be further separated into "lithogenic" and "anthropogenic" components using Ti as an indicator of the concentration of lithogenic-derived aerosols supplied by rock weathering:

$$[Pb]_{lithogenic} = [Ti]_{sample} \times [Pb/Ti]_{Earth's\ Crust} \qquad (ii)$$

Notice that for most samples, the total Pb flux and anthropogenic Pb flux are nearly identical because the concentrations of lithogenic Pb are so low. Both the atmospheric Pb flux in DK (Fig. 5b) and the relative importance of anthropogenic Pb (Fig. 5c) have been declining since the 1950's (Fig. 5b).

3.7. Isotopic Composition of Pb in Peat from GL and DK

The concentrations of Pb measured in the leachable and residual fractions, as well as the isotopic composition of this Pb (summarized as the [206]Pb/[207]Pb ratio), are shown in Figure 6. The large difference in total Pb concentrations between the DK
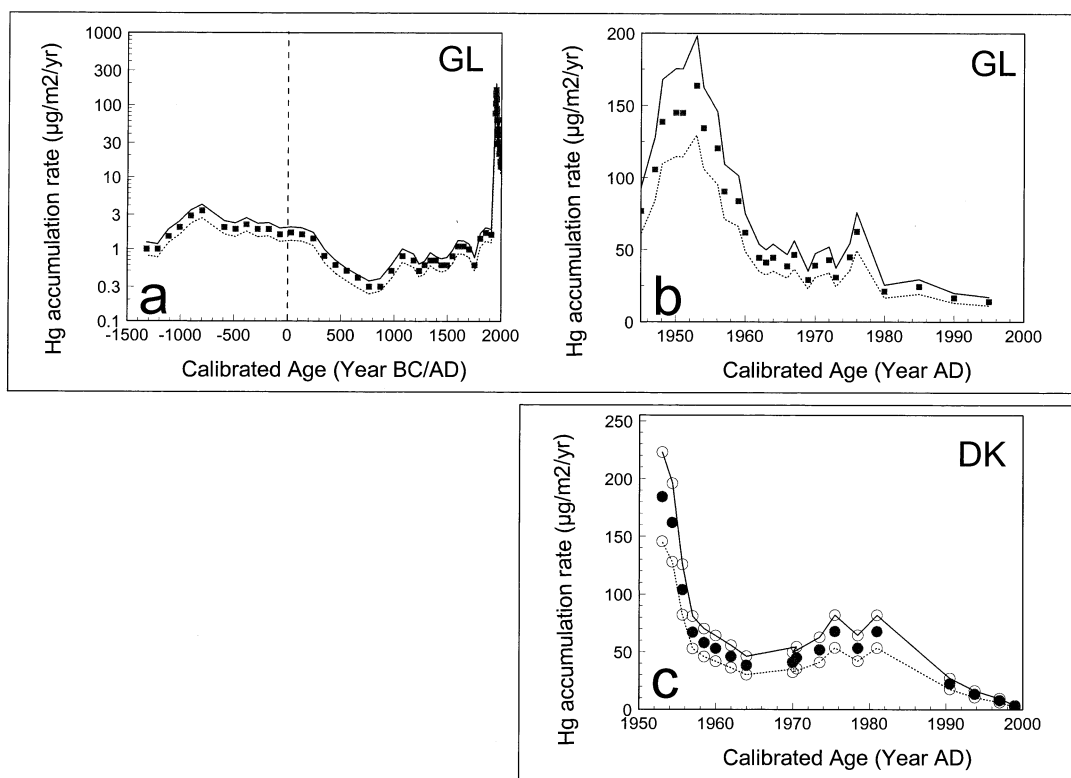
Fig. 4. Mercury accumulation rates (μg/m^2/yr). a) GL, all samples. b) GL (samples dated using the bomb pulse curve for [14]C. The upper solid line represents the estimated flux + 20%, the lower line the estimated flux − 20%. c) DK samples dated using the bomb pulse curve for [14]C. The upper empty symbols represent the estimated flux + 20%, the lower hollow symbols the estimated flux − 20%.

and GL cores described earlier (seen in the "A" cores which were measured using XRF and presented in Fig. 5a) is also seen in the "B" cores where Pb concentrations were measured in selected samples using IDMS (Fig. 6a,b). However, the leaching study undertaken using TIMS indicates two additional features. First, the abundance of "leachable" Pb tends generally to be more abundant than the "residual" Pb (except for two samples from GL). In the DK core in particular, the predominance of leachable Pb is most clearly associated with the samples containing the highest total Pb concentrations (Fig. 6a), with the highest concentration found at 15–16cm (141.4 μg/g Pb in the leachable fraction, and 32.1 μg/g Pb in the residual fraction). For comparison with these concentrations, the "natural background" concentration of Pb in preanthropogenic peats in Switzerland dating from ca. 8000 to 5000 ^{14}C yrs BP is approximately 0.2 μg/g Pb, and this difference indicates in a general way the extent to which the DK core has been contaminated by industrial Pb. The isotopic composition of Pb in the two fractions, summarized here as the [206]Pb/[207]Pb ratio (Fig. 6b), is virtually identical and this clearly demonstrates a common origin of the Pb in both fractions. One possible explanation of the similarity in Pb isotopic composition in each of the DK peat fractions is that anthropogenic Pb supplied by various industrial emissions has been scavenged by soil-derived aerosols supplied by crustal weathering, such that the "soil dust signature" has been overprinted by anthropogenic Pb. A second possible explanation is that the

"residual" fraction obtained by the extraction procedure has included some of the "leachable" Pb supplied primarily by anthropogenic sources.

Second, the isotopic composition of Pb in the two peat cores is very different, with the GL samples being far more radiogenic (Fig. 6b). The pattern in [206]Pb/[207]Pb in the DK core is remarkably similar to the temporal variation in [206]Pb/[207]Pb seen in four peat profiles from Switzerland (Weiss et al., 1999a), as well as the record of [206]Pb/[207]Pb reported for *Sphagnum* moss samples from the University of Geneva herbarium (Weiss et al., 1999b). The ratio [206]Pb/[207]Pb in the Upper Continental Crust (Kramers and Tolstikhin, 1997) as well as in preanthropogenic (dating from 8000 to 5300 ^{14}C yr BP), atmospheric aerosols from Switzerland (Shotyk et al., 2001), is approximately 1.2. All of the measured values from the DK core are significantly less radiogenic than this, indicating that anthropogenic Pb has dominated the atmospheric Pb inputs to the DK bog.

3.8. Predominant Sources of Anthropogenic, Atmospheric Pb and As in Denmark

The lithogenic Pb fraction derived from atmospheric soil dust can be estimated as the product of the Ti concentrations of the DK profile, and the Pb/Ti ratio of the Earth's Crust (Wedepohl, 1995); this assumes that lithogenic Pb is derived exclusively from atmospheric soil dust, and that the Pb/Ti ratio of
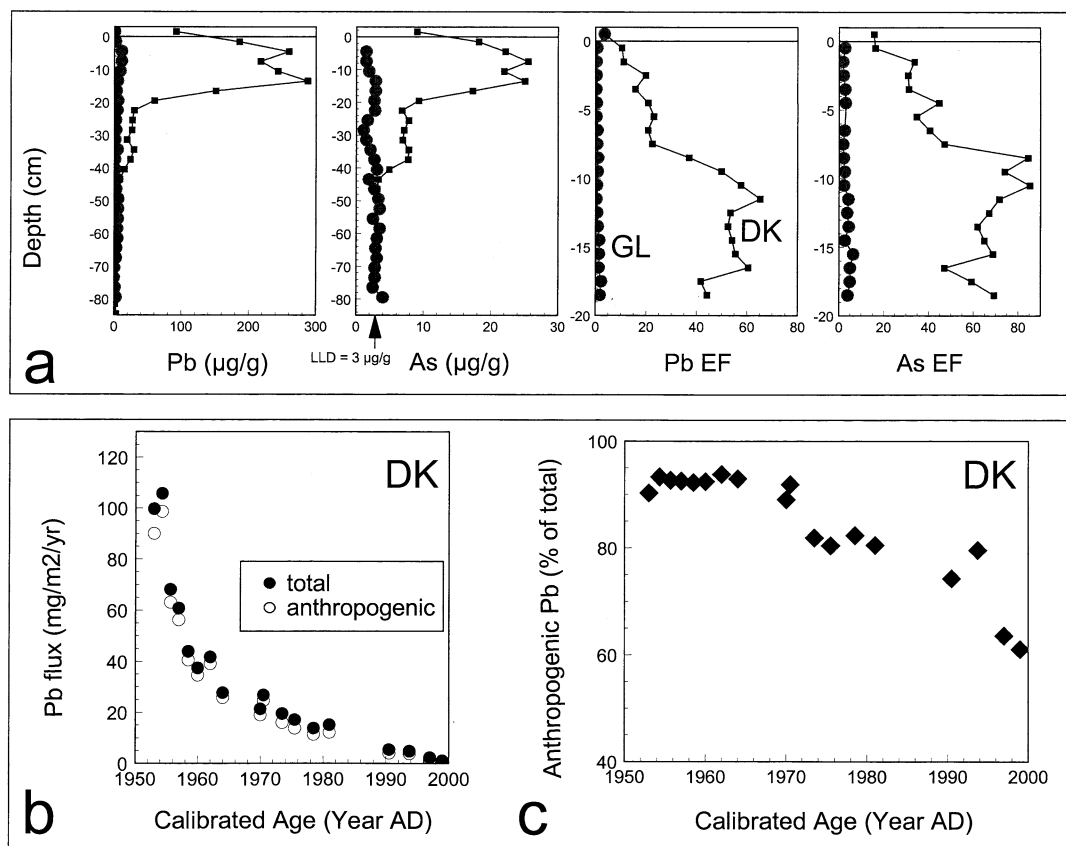
Fig. 5. a) Pb and As concentrations (μg/g)in the GL and DK cores, and the Pb and As EFs calculated as described in the text. There is no measurable enrichment of Pb or As in the surface layers of the GL core. Age dates of the deepest samples from these "A" cores obtained using [14]C (decay counting, University of Berne) which yielded GL (>78cm) 3540 ± 30 ^{14}C yr BP and DK (>84cm) 2790 ± 40 ^{14}C yr BP (conventional radiocarbon yrs BP). b) the atmospheric fluxes of total Pb (solid symbols) and anthropogenic Pb (hollow symbols) in DK, obtained as described in the text. c) the percentage of anthropogenic Pb and its temporal evolution in DK.

this dust is similar to that of the Earth's Crust. Using the Ti concentrations which are available for the top 20 cm of the "B" cores, the "lithogenic" Pb component has been calculated (Fig. 6c) and in all cases, it is small even compared to the "residual" Pb fraction measured using TIMS. The lithogenic Pb fraction of the DK peat profile has also been estimated using Zr as the conservative, lithogenic reference element, but the outcome is much the same (Fig. 6c).

One disadvantage of this approach is that the Pb/Ti and Pb/Zr ratios of atmospheric soil dust may not be identical to the corresponding values for the Earth's Upper Crust (UC) as reported by Wedepohl (1995). In an earlier paper of a Swiss peat bog profile, we found that the "background" Pb/Sc ratio in preanthropogenic aerosols dating from ca. 5000 to 8000 ^{14}C yr BP was approximately 4× the value presented by Wedepohl (1995) for the UC (Shotyk et al., 1998). To take into account these findings, we have also calculated the concentrations of "lithogenic" Pb for the DK core using "background" values of Pb/Ti = 4× UC (Fig. 6c). However, even taking the value of Pb/Ti = 4× UC, the theoretical "lithogenic" Pb component in many samples is still ca. one half of the concentrations measured in the "residual" fraction. The differences between the "residual"

fraction measured using TIMS and the "lithogenic" fraction calculated using Pb and Ti (or Zr) concentrations indicate that further studies are needed to better quantify the isotopic composition of the "natural" Pb component of peats which are impacted by anthropogenic Pb.

Using the concentrations of Ti, Pb, and As, it is possible to estimate the contribution of anthropogenic Pb and As to the inventories of these elements in the DK peat core, because the "lithogenic" Pb or As fraction is small compared to the total concentrations. Taking Ti as an indicator of the concentration of aerosols supplied by rock weathering, the concentration of Pb (or As) which was supplied to the bog via atmospheric deposition of soil-derived aerosols can be estimated using Eqn. (ii). Here, we have calculated the "lithogenic" Pb component using both Pb/Ti = UC and Pb/Ti = 4× UC (Fig. 6c). With respect to As, we recently reported As/Sc ratios for preanthropogenic, atmospheric aerosols (for the same Swiss bog, and the same period of time as for Pb/Sc) which are approximately 10× the ratio for the UC (Shotyk et al., 2002a); here, therefore, we have calculated "lithogenic" As using both As/Ti = UC and As/Ti = 10× UC (Fig. 6c). Once the lithogenic Pb (or As) component has been quantified, anthropogenic Pb (or As) is calculated as
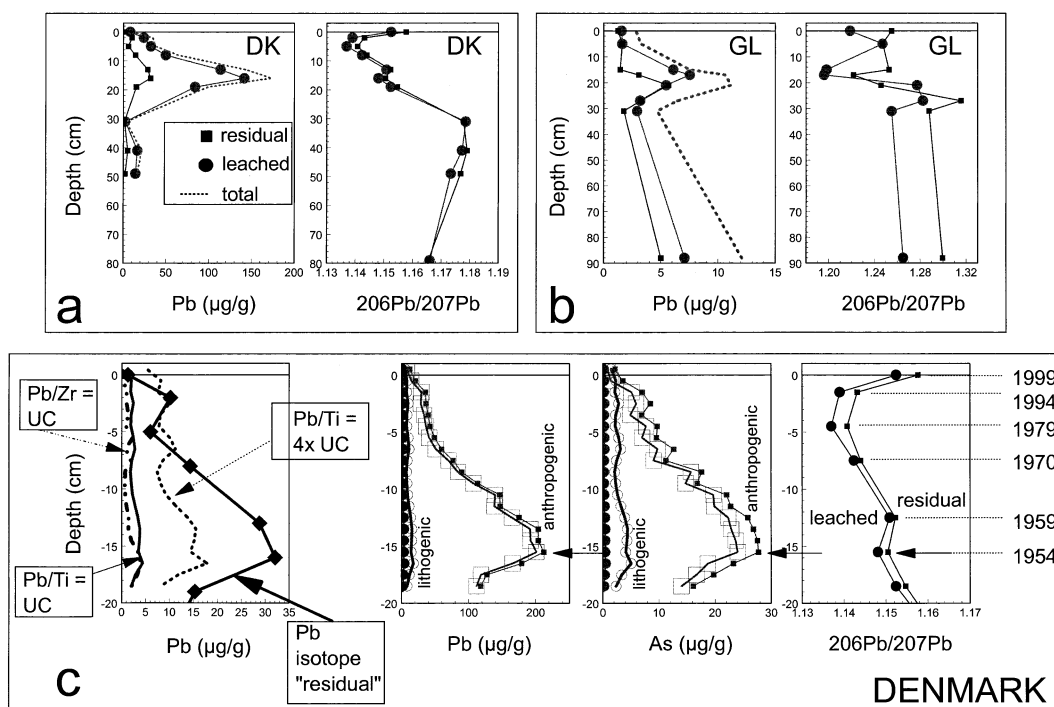
Fig. 6. a) Pb concentrations and the isotopic composition of Pb in the exchangeable and residual fractions of the "B" cores from DK. b) Pb concentrations and the isotopic composition of Pb in the exchangeable and residual fractions of the "B" cores from GL. c) "Residual" Pb measured using the extraction procedure described in the text, compared with "lithogenic Pb" calculated using either Pb/Zr = UC, Pb/Ti = UC, or Pb/Ti = 4× UC. Also shown are "lithogenic" Pb and As calculated using either Pb/Ti = UC or 4× UC, and As/Ti = UC or 10× UC, in relation to the ^{206}Pb/^{207}Pb ratio of selected samples, and selected age dates obtained using ^{14}C (atmospheric bomb pulse). The small arrows point to the maximum concentration of Pb and As which was dated to AD 1954.

$$[Pb]_{anthropogenic} = [Pb]_{total} - [Pb]_{lithogenic} \qquad (iii)$$

The calculated values for lithogenic and anthropogenic Pb and As calculated in this way are shown in Figure 6c, along with a graph of the ratio ^{206}Pb/^{207}Pb, and selected ^{14}C age dates (Table 2). Notice that both sets of calculations for each element indicate that the anthropogenic component dominates the Pb and As inventories in this section of the DK core.

The maximum concentration of anthropogenic Pb and As is found in peats dating from 1954; this matches the maximum flux of atmospheric Hg (Fig. 2b and Fig. 4c), and suggests a common source: this is most likely coal, as coal is commonly enriched in all three of these elements (Bouska, 1981; Valkovic, 1983; Swaine, 1990); Zn (not shown) is also clearly enriched at this depth. The data presented here (Figs. 2b, 4c, and 6c) suggest that the maximum extent of atmospheric Pb, As, and Hg contamination in Denmark had already peaked in 1954, and has more or less declined ever since. It is noteworthy that the Clean Air Act was passed in the U.K. in 1956, primarily to reduce the industrial emission of particulates and gases from burning coal. Given that the industrial heartland of the U.K. is nearly due west of Denmark and that the predominant wind direction is from west to east, British coal burning is likely to be an important, if not predominant source of these contaminants. According to the compilation published by Farmer et al. (1999), British coal consumption peaked in the early 1950's.

Taken together, it appears that the changing accumulation rates of anthropogenic Hg, Pb and As revealed by the DK peat core may reflect to a large extent the history of the British coal industry and the chronology of the Second Industrial Revolution.

To further evaluate the possible link between these contaminants and British coals, the ratio ^{208}Pb/^{206}Pb has been plotted against the ^{206}Pb/^{207}Pb values (Fig. 7). Clearly, the DK peat samples are much closer in isotopic composition to the values for British coals (Farmer et al., 1999) than they are to the values for U.K. gasoline leads (Monna et al., 1997). Thus, the Pb isotope data, combined with the chronology of the enrichments in Hg, Pb and As concentrations, suggest that coal burning was the main source of these contaminants to the DK peat profile.

In samples above ca. 20 cm in the DK profile, there is a sharp shift (after AD 1959) toward much less radiogenic values ^{206}Pb/^{207}Pb (Fig. 6c) which reflects the growing importance of leaded gasoline contributions; the ores used to synthesize alkyllead compounds for gasoline such as Pb from the Broken Hills mine of Australia, have had ^{206}Pb/^{207}Pb values as low as 1.04. The most recent sample in the profile (AD 1999) shows significantly more radiogenic values, compared to the 1970's, clearly reflecting the reduction in gasoline Pb concentrations, and the eventual phasing-out of leaded gasoline in Europe; this change is also seen in four
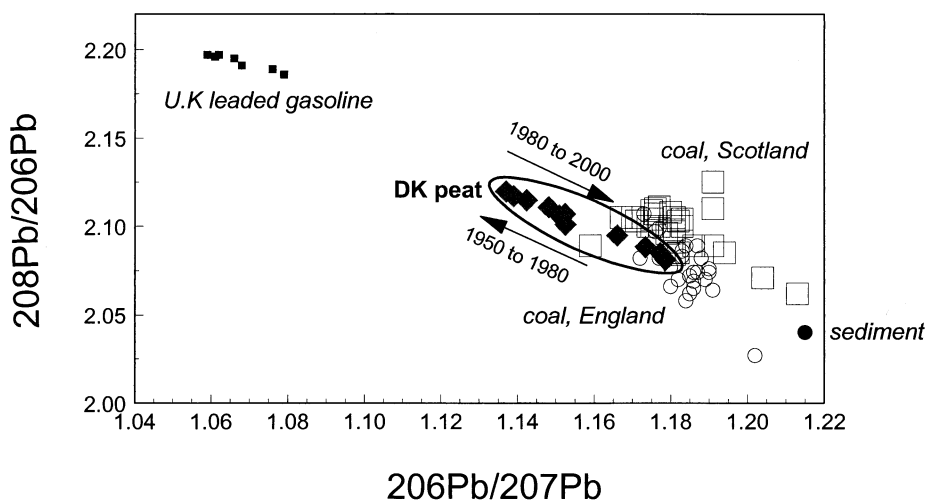
Fig. 7. Plot of $^{208}Pb/^{206}Pb$ versus $^{206}Pb/^{207}Pb$ for the leached fraction of the DK peat samples (Table 3). U.K. coal (from Farmer et al., 1999) and U.K. leaded gasoline (from Monna et al., 1997). Also shown is the isotopic composition of Pb in an Oxfordian sediment (from Shotyk et al., 1998). The direction of the arrows illustrate the temporal evolution of atmospheric Pb in DK from 1950 to 1980 (towards less radiogenic values as gasoline lead grows in importance) and from 1980 to 2000 (toward more radiogenic values as gasoline lead consumption declines).

peat profiles from Switzerland (Weiss et al., 1999a, Shotyk et al., 2003), as well as the record of $^{206}Pb/^{207}Pb$ reported for *Sphagnum* moss samples from the University of Geneva herbarium (Weiss et al., 1999b). It is important to emphasise that the *decline in anthropogenic Pb concentrations* (starting in 1954) which is shown in Figure 6c *predates by approximately 25 yr the minimum in* $^{206}Pb/^{207}Pb$; the minimum in this Pb isotope ratio corresponds to the maximum impact in gasoline Pb emissions (Shotyk et al., 2002b). As noted earlier, this decline in $^{206}Pb/^{207}Pb$ was caused by the introduction of gasoline leads of Australian origin with very low $^{206}Pb/^{207}Pb$ values. The minimum $^{206}Pb/^{207}Pb$ value (in 1979) is consistent with production records which indicated leaded gasoline consumption in Europe reached its zenith in 1980 (Hagner, 2000). Moreover, direct air Pb measurements in Denmark document strong declines in Pb concentrations since the late 1970's (Jensen and Fenger, 1994). However, there appears to be no published air Pb data older than ca. 1970. The Pb isotope results presented in Figure 6c are significant, as they show that the greatest percentage of anthropogenic Pb recorded by the peat profile in DK was not caused primarily by leaded gasoline consumption, but rather from coal-burning and other industrial sources. Moreover, these results show that anthropogenic Pb went into decline well before either the introduction of maximum allowable Pb concentration in gasoline (in 1978 in the EU according to Hagner, 2000), or the ban on leaded gasoline sales in the EU in 1987 (Hagner, 2000). While leaded gasoline certainly contributed to a pronounced shift in the isotopic composition of Pb-bearing aerosols, other sources of anthropogenic Pb were quantitatively more important in DK during the first half of the 20th century. Similar conclusions were drawn from a recent study of duplicate peat cores from a Swiss bog which showed a maximum in Pb EF predating the minimum in $^{206}Pb/^{207}Pb$ (Shotyk et al., 2002b).

4. DISCUSSION

4.1. Natural Sources of Hg to the Minerotrophic GL Core

The elevated Hg concentrations in the uppermost layers of the GL core are effectively contemporaneous with those of the DK core (Fig. 2) which has received Hg solely from atmospheric deposition. Given the fundamental differences in the hydrology and geochemistry of the two sites (ombrotrophic, acidic bog in DK, minerotrophic, alkaline fen in GL), and the differences in peat accumulation rates (Fig. 3), it is unlikely that natural processes could have caused such a similar chronology of atmospheric Hg. The most likely explanation for the elevated Hg concentrations in the surface layers of the GL profile, therefore, is the changing rates of anthropogenic emissions of Hg to the atmosphere during the past century. However, the possible importance of other sources of Hg to the GL core also requires consideration.

4.1.1. Atmospheric soil dust

The concentrations of mineral matter in peat profiles may vary because of temporal changes in atmospheric soil dust deposition rates, organic matter decomposition, or both. Titanium, Zr, and Y are conservative, lithogenic elements in the sense that their oxides and silicates are resistant to chemical weathering, and their distribution in the peat profiles reflects the abundance of mineral material (Fig. 8a). Rubidium is found primarily in K feldspar where it substitutes for K, and its distribution in the profile generally resembles that of Zr and Y (Fig. 8a); Rb too, therefore, provides an indication of the abundance and distribution of mineral matter in the profile. In the DK profile, the measured values of these elements are in a range typical of ombrotro-
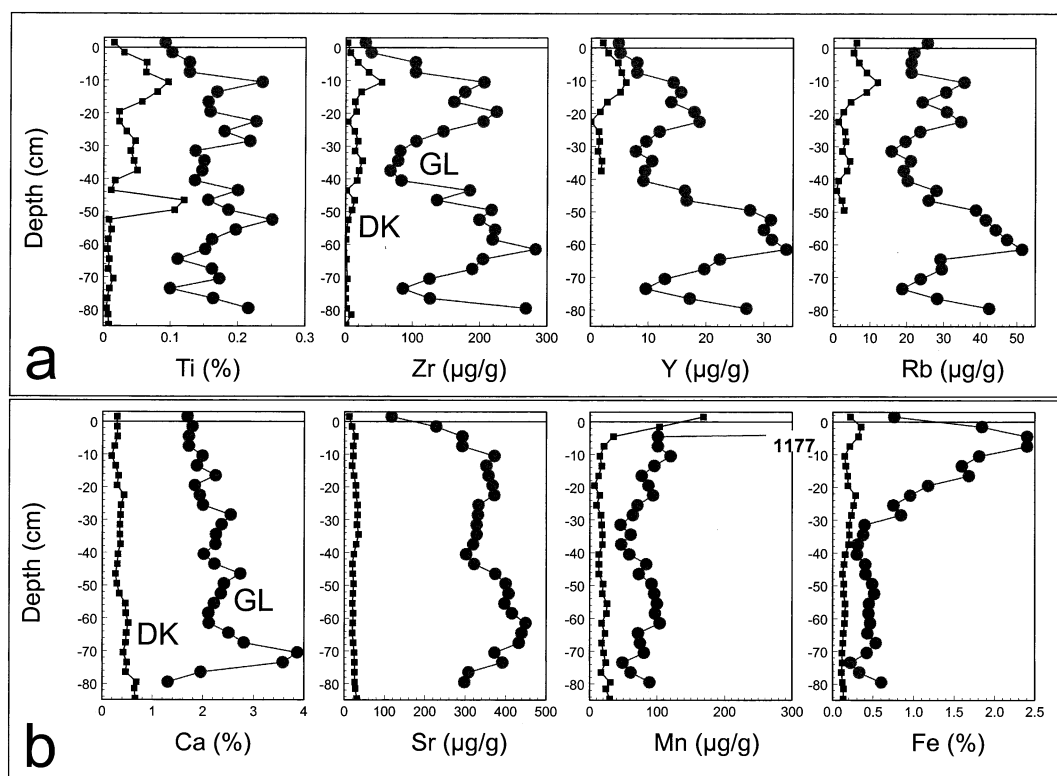
Fig. 8. a) Ti (%), Zr, Y and Rb (μg/g) concentrations in the GL (green) and DK (red) "A" cores (3 cm slices). b) Ca (%), Sr, Mn (μg/g), and Fe (%) concentrations in the GL and DK "A" cores (3 cm slices).

phic bogs which receive minerals exclusively from atmospheric soil dust (Shotyk et al., 2001). In contrast, these elements are typically 5× more abundant in the minerotrophic GL profile (Fig. 8a) core. Assuming that the lowest concentrations of Hg in the GL profile (1.6 ng/cm³ at 47 cm) represent pre-Industrial, "background" values, the maximum concentration (24.0 ng/cm³ at 21 cm) exceeds this value by 15×. This concentration difference greatly exceeds the variation in Zr concentrations over the same distance (1.6× as shown in Fig. 8a). Therefore, the variation in mineral matter supply (e.g., from changes in the flux of atmospheric soil dust) is not a viable explanation of the magnitude of the variation in Hg concentrations with depth.

4.1.2. Marine aerosols

The porewaters of the GL and DK cores typically contain ca. 10 mg/L Cl⁻, compared to continental ombrotrophic peat bogs from Switzerland which average ca. 0.3 mg/L Cl⁻ (Steinmann and Shotyk, 1997). While the elevated chloride concentrations in the GL and DK porewaters reveal the influence of sea salt spray at both locations, and while this may be a natural source of Hg to the cores, the relative importance of this source must have been relatively constant over time. Thus, atmospheric deposition of marine aerosols cannot explain the change in Hg concentrations with respect to depth and time seen in both peat profiles (Fig. 2).

4.1.3. Aquatic inputs via chemical weathering of local soils and rocks

The low abundance of Ca and Sr (Fig. 8b) in the DK core (average 0.40% and 25.7 μg/g, respectively) is typical of ombrotrophic bogs (Shotyk et al., 2001) which receive inputs exclusively from the atmosphere. In contrast, the higher Ca and Sr concentrations in the GL core (average 2.2% and 347 μg/g, respectively) demonstrate extensive rock-water interaction characteristic of minerotrophic mires (Fig. 8b). Similarly, Mn and Fe are much more abundant in the GL profile (Fig. 8b). The relatively high pH of the waters combined with the abundance of Ca and Sr in the peats indicates active dissolution of carbonate minerals, either in the sediments underlying the peat, in the watershed, or both (Shotyk, 2002). The elevated Mn concentrations in the surface layers of both cores may either be due to plant uptake and recycling, oxidation, or both. Iron concentrations are very high in the GL profile, and are strongly enriched in the uppermost layers: this is most likely a redox-related transformation (Steinmann and Shotyk, 1997) as the Fe concentrations are well in excess of the concentration required by growing plants. Like Ca and Sr, the Mn and Fe which have been supplied to the GL profile may originate in carbonate mineral phases in the surrounding rocks and underlying sediments (Andersen, 1997). However, between 47 and 21 cm where the Hg concentrations increase by 15×, there is no change in the Sr concentrations (Fig. 8b). Thus, weathering of
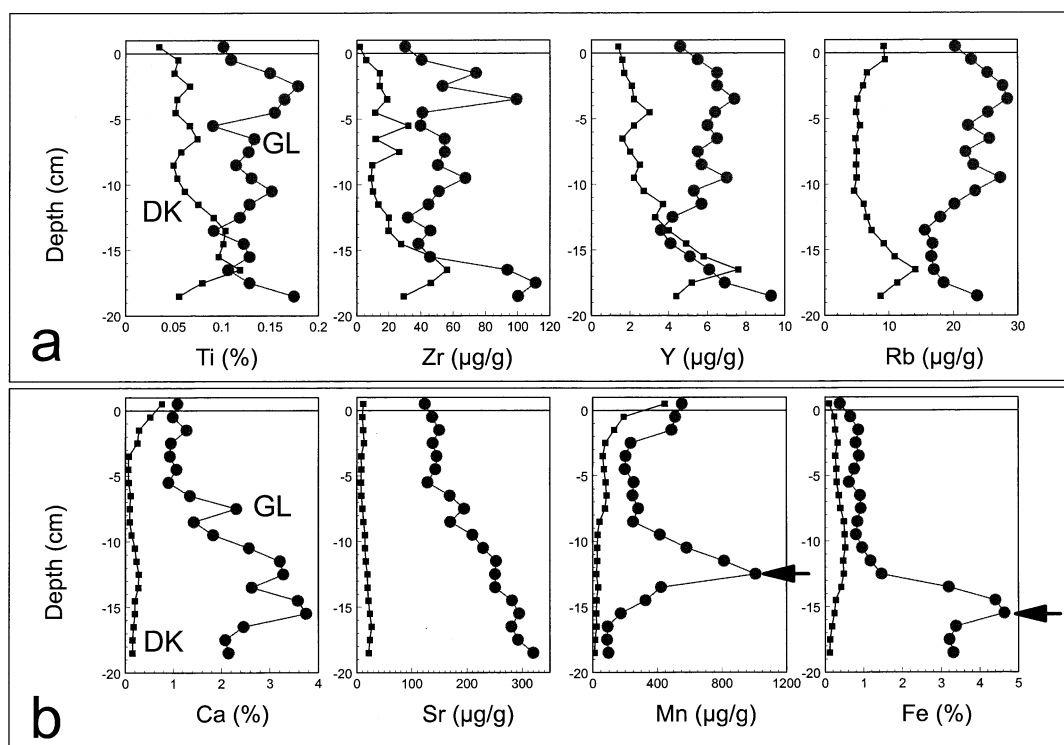
Fig. 9. a) Ti (%), Zr, Y and Rb (μg/g) concentrations in the GL (green) and DK (red) "B" cores (1 cm slices) b) Ca (%), Sr, Mn (μg/g), and Fe (%) concentrations in the GL and DK "B" cores.

local rocks and soils cannot explain the increasing Hg concentrations in the uppermost, recent layers of the GL peat profile.

4.2. Natural Geochemical Processes and Their Effects on Hg in the Minerotrophic GL Profile

4.2.1. Decomposition of organic matter

The bulk density of the samples at 47 and 21 cm in the GL profile differ only by a factor of 1.7× (Fig. 2a), in contrast with the differences in Hg concentrations (15×). We assume that the bulk density of a given type of peat is a reflection of the extent of its decomposition (degree of humification). Support for this assumption comes from a detailed spectroscopic characterisation of organic matter in the Swiss peat bog profile at Etang de la Gruère (Cocozza et al., 2003). Bulk density, therefore, helps to take into account any changes in metal concentrations which take place during the decomposition of organic matter. In a recent paper about Hg accumulation rates in peat cores from Patagonia, Biester et al. (2003) suggested that bulk density is not an adequate parameter to express changes in peat humification, and that Hg accumulation rates (calculated as we have described here) should be corrected for humification to take into account mass loss during decay. However, in the GL peat profile, the difference in bulk density at 47 versus 21 cm (1.6×) is similar to the difference in Zr concentrations (1.7×). Zirconium is a conservative element which resides almost exclusively in zircon, and this element (along with other conservative trace metals) should increase in concentration with increasing extent of peat decay. In fact, the differences in Zr

concentrations are comparable to the differences in bulk density; taken together these data suggest that the differences in humification alone cannot explain differences in Hg concentrations by more than a factor of two. As a consequence of these data and arguments, it is unlikely that physical processes such as organic matter decomposition can explain the magnitude of the variation in Hg concentrations with depth in the GL profile.

4.2.2. Redox-related processes in the oxic zone

It has been suggested that redox-related transformations of Fe and Mn in marine and lacustrine sediments may contribute to Hg enrichments in the surface layers of these sediments. For example, Hg may become adsorbed onto Fe and Mn oxides which are formed when Fe (II) and Mn (II) in the anoxic zone diffuse upward and become oxidized (Gobeil et al., 1999). Asmund and Nielsen (2000) have summarised some of these studies, and document very strong correlations between Mn and Hg or Fe and Hg in some lake sediment cores. While peatlands do not have an overlying water column for Mn and Fe to diffuse into, they may have a shallow oxic zone, depending on the depth to water table which varies seasonally (Shotyk, 1988). The shapes of the Mn and Fe concentration profiles in the GL core (Fig. 8b) suggest that there may be some oxidation of Fe and Mn in the surface and near surface layers. To help evaluate the possible importance of this process on the Hg concentration profile, samples from the uppermost 20 cm of the "B" cores (1 cm slices) were also measured for trace elements, including Mn and Fe, using XRF (Fig. 9). Except for the
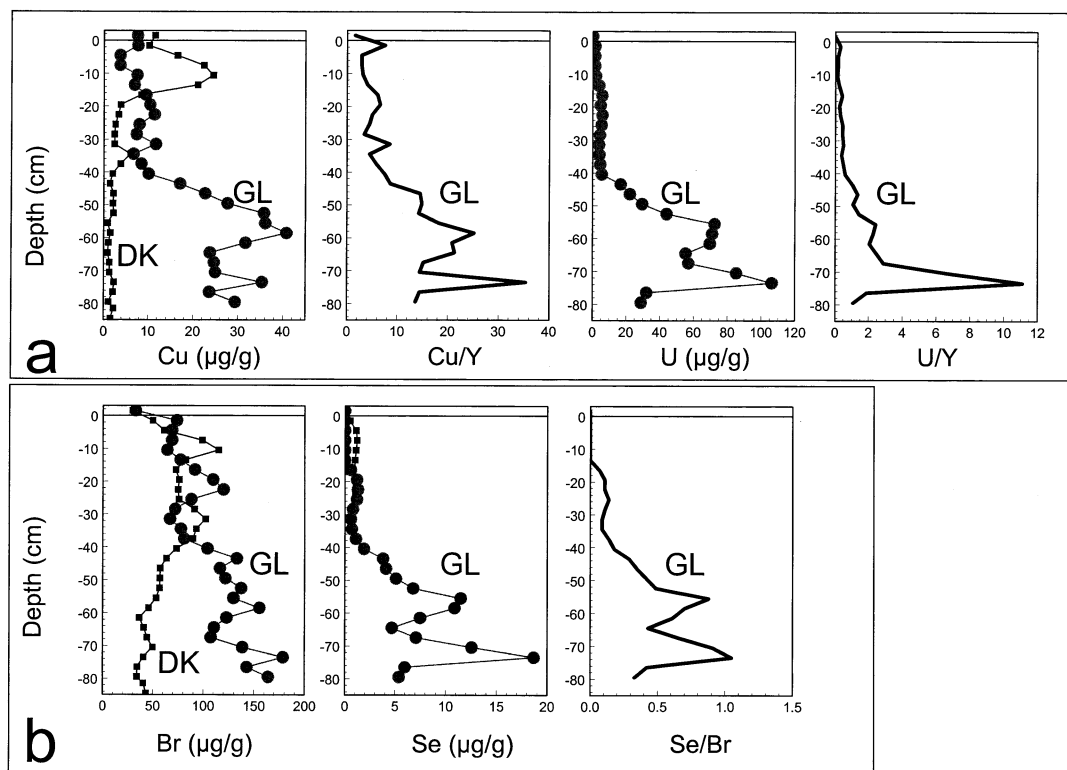
Fig. 10. a) Cu and U concentrations (μg/g), and Cu/Y and U/Y rations in the GL (green) and DK (red) "A" cores. b) Br and Se concentrations (μg/g) in the GL and DK "A" cores, and the Se/Br ratio.

elevated Mn concentration in the top layers at DK, the DK core reveals no peak in either element. In contrast, the GL core shows a pronounced enrichment of Mn at 12–13 cm, and Fe at 15–16 cm (arrows in Fig. 9). However, these Mn and Fe peaks are well above the peak in volumetric Hg concentrations which is found in the GL core between 20 and 25 cm (Fig. 2a). The elevated Hg concentrations beginning at ca. 25 cm at GL, therefore, is independent of those of Mn and Fe, suggesting that redox-related transformations of Mn and Fe have not noticeably affected Hg. While redox-related transformations of Mn and Fe are probably operating within the peat profile, there have been no observable effects of these changes on the Hg profile. The elevated Hg concentrations in the near surface layers, therefore appears to be mainly influenced by atmospheric deposition. Thus, even in the minerotrophic peat profile at GL, the Hg concentration profile appears to provide a record of the changing rates of atmospheric Hg deposition.

4.2.3. Redox-related processes in the anoxic zone

Mercury is highly enriched in all of the peat layers below 50 cm of the GL peat profile, compared to the lowest concentrations in the middle of the core (Fig. 2a). As these samples are more than one thousand years old, natural geochemical processes must be invoked to explain the Hg enrichments. Copper concentrations are also elevated in the deeper layers of the GL core, and the Cu/Y ratio illustrates the pronounced enrichment of this metal with increasing depth (Fig. 10a). Similarly, U concentrations reach more than 100 μg/g (Fig. 10a) which is

ca. 50× crustal abundance and 2000× the concentration found in ombrotrophic peats. Again, normalising the U concentrations to Y, the U/Y ratio reveals the shape of the U enrichment (Fig. 10a). Both Cu and U are commonly enriched in anoxic, minerotrophic peats due to reductive dissolution Cu(II) to Cu(0) and U(VI) to U(IV), respectively (Shotyk, 1988). The zone of maximum Cu and U enrichment is found in the limnic peat layer made up predominately of the remains of aquatic plants just above the basal sediment; previous studies also revealed enrichments of Cu and U in this zone of some Canadian bogs (Shotyk et al., 1992).

Bromine and Se are both supplied to these peatlands from sea salt spray, but the Se/Br ratio (Fig. 10b) indicates that the deeper peat layers at GL are preferentially enriched in Se. While the variations in Br concentrations can largely be explained in terms of the decay of organic matter, this process alone cannot explain the large increase in Se concentrations with depth through the GL profile. The general shape of Se (Fig. 10b), however, resembles that of U and Cu/Y (Fig. 10a), suggesting that a redox-related process has contributed to the Se enrichment. The pronounced enrichments of Cu and U (as evident by their ratios to Y) and Se (revealed by comparison to Br) at the same depths as the enrichment of Hg (Fig. 2b) suggest that the natural Hg enrichments in the deeper peat layers of the GL profile are related to redox transformations. The details of this process, however, are unclear. Given that the solubility product constant of Hg selenide (K_{sp} = 10^{-62}) is orders of magnitude lower than even that of Hg sulphide (K_{sp}

$= 10^{-52}$), it may be that Se has played a direct role in the natural enrichment of Hg toward the bottom of the GL profile.

4.3. Comparison with Marine and Lacustrine Sedimentary Records of Hg Accumulation

Age dated lake sediments from across the Arctic have been measured for Hg and the ratio of postindustrial to preindustrial Hg accumulation rates were found to be in the range 0.7 to 9 (Landers et al., 1998). The authors admit, however, that their study was hampered in many cases by local metal sources contributing to high background values: this is a fundamental problem with lake sediment archives, as metals are supplied by atmospheric as well as non-atmospheric sources. In cases where "background" values are elevated due to natural, geo-chemical sources, the additional impact of anthropogenic Hg may be difficult to detect. Asmund and Nielsen (2000) studied Hg in marine sediments from Greenland, and found that Hg fluxes had increased only by a factor of two, compared to the values for sediments from the previous century. Bindler et al. (2001) examined many lake sediment profiles from Greenland, and reported concentration increases of only 2 to 3 × from preindustrial to postindustrial times. In each of these cases, however, the measured Hg accumulation rates reflect not only atmospheric inputs, but also inputs to the sediments from the entire watershed (from physical and chemical weathering) as well as focusing processes within the sedimentary basin. In contrast, the GL peat profile studied here provides the first long-term record of *atmospheric* Hg accumulation in Greenland. Because the surface peat layers receive Hg only from the air, it provides a much more sensitive record of changes in atmospheric deposition. This sensitivity is revealed by the difference between the background fluxes which are as low as 0.3 to 0.5 $\mu g/m^2/yr$ (AD 550 to 975) and the maximum flux of 164 $\mu g/m^2/yr$ (AD 1953). In sediment records, these extreme values are masked by the continuous input of Hg from non-atmospheric sources. In fact, peat bogs are probably the most sensitive continental archives of atmospheric Pb and Hg deposition, and may serve as archives of many of other trace elements of contemporary environmental interest.

4.4. Implications for the Global Atmospheric Hg Cycle

A model of the global atmospheric Hg cycle has recently been published (Lamborg et al., 2002) in which an annual preindustrial flux of Hg to the continents of 4 Mmoles was reported. If this value is taken to represent the continental land mass (total 147×10^6 km^2), then an average, preindustrial flux of 5.5 $\mu g/m^2/yr$ is implied. For comparison, the minimum preindustrial flux recorded by the GL core is only 0.3 $\mu g/m^2/yr$; this is also the minimum Hg accumulation rate recorded by the Swiss peat bog (Roos-Barraclough et al., 2002a). In fact, the value reported by Lamborg et al. (2002) is at the upper end of the range (0.3 to 8 $\mu g/m^2/yr$) reported for the Swiss bog (Roos-Barraclough et al., 2002a), with the uppermost Swiss values seen only during periods of volcanic activity. The modelled result is also outside of the preindustrial range reported here for GL (0.3 to 3 $\mu g/m^2/yr$). Given that the deeper GL peats containing elevated Hg accumulation rates are enriched in Cu, Se, and U, we assume that the lowest Hg accumulation rates

(0.3 to 0.5 $\mu g/m^2/yr$ from AD 550 to 975) are representative of the preindustrial, atmospheric Hg flux. The preindustrial flux calculated by Lamborg et al. (2002), therefore, may be too large by as much as one order of magnitude.

At this time, we cannot determine how much of the atmospheric Hg accumulation in GL may have been due to long range atmospheric transport, and how much due to local sources. Since our study began, we have learned that the U.S. military operated a secret base called "Bluie West One," across the fjord from the sampling site, from 1941 to 1958 (the former airfield is now Narsarssuaq airport). This base is said to have housed up to 10000 persons during its zenith, and had its own kilns for manufacturing bricks: this may help to explain the magnitude and chronology of the elevated Hg fluxes from this period. Additional studies of peat bogs from other locations should help improve our understanding of local and long-range Hg transport, and further improve our knowledge of preindustrial and postindustrial Hg accumulation rates.

4.5. Temporal Changes in the Isotopic Composition of Pb in Greenland

As noted earlier, Pb concentrations are far lower in the GL core compared to DK. The Pb EF calculated using the Pb and Ti concentrations failed to reveal a significant enrichment of Pb in the surface layers of the GL core (Fig. 5a). However, in the surface and near-surface peat layers at GL, the Pb is much less radiogenic in both the leachable and residual fractions (Fig. 6b), compared to deeper, older peat layers. Given that this zone dates from the past century, the shift in Pb isotope ratios probably reflects the input of anthropogenic Pb with lower $^{206}Pb/^{207}Pb$ ratios. Anthropogenic, atmospheric Pb in Greenland has previously been shown to be derived primarily by gasoline lead used in North America (Rosman et al., 1998). Alklyllead compounds in N. America were synthesized primarily using lead ores of the Mississipi Valley type deposits which are much more radiogenic ($^{206}Pb/^{207}Pb$ ca. 1.2) compared to the ores used for gasoline lead in Europe. However, even these, relatively radiogenic leads are considerably less radiogenic than the rocks and minerals of Greenland ($^{206}Pb/^{207}Pb$ up to 1.3 in Fig. 6b). Thus, addition to the surface peat layer at GL of Pb derived from N. American gasoline lead, could easily have caused the significant decrease in $^{206}Pb/^{207}Pb$ revealed by the peat core. The shift in $^{206}Pb/^{207}Pb$ to less radiogenic values in samples above ca. 20 cm in the GL core (Fig. 6b), therefore, most likely reflects the addition of Pb derived from the combustion of leaded gasoline in N. America. Thus, while total Pb concentrations and their ratio to Ti failed to indicate an anthropogenic impact, the Pb isotope data clearly does. Additional work is required with respect to leaching techniques such as those now being used to fractionate Pb in soils (Harlavan and Erel, 2002; Emmanuel and Erel, 2002), with the goal of improving the recovery of the atmospheric Pb component which has been supplied by anthropogenic emissions.

The Pb concentrations in the leachable fraction generally exceed those of the residual fraction, even in the deeper peat layers dating from preanthropogenic times (Fig. 6b). In the deepest peat samples studied (88cm), the leached and residual fractions are isotopically different: both fractions are highly radiogenic which suggests that both sources are local. Many

geological studies employing leaching techniques indicate that radiogenic Pb in minerals is more easily recovered in the "acid-leachable" fraction because Pb is found in radiation lattice defects where it is less strongly held, compared with lattice-bound Pb which was originally incorporated in U-Th-bearing minerals. In the GL samples, however, it is the residual fraction which is more radiogenic than the leachable fraction. Given that this section of the peat profile is strongly minerotrophic, the most obvious possible sources of Pb include i) physical incorporation of fine grained mineral matter by the plants which were growing at the time peat formation began (ca. 3000 ^{14}C yr BP), and ii) chemical adsorption/complexation of dissolved Pb which had been released to the plants and basal peat by chemical weathering of the host minerals. While it may be that the former process is primarily responsible for the isotopic composition of the Pb in the more radiogenic "residual" fraction, and the latter for the less radiogenic Pb in the "leachable" fraction, there are other possibilities. For example, to some extent the "leachable" fraction is an artefact of leaching the samples for 2 h in 2N HCl which would not only remove exchangeable Pb, but also dissolve some fine grained mineral phases hosting Pb such as micas and feldspars; some of these may ultimately have been supplied by atmospheric soil dust and would therefore be less radiogenic.

The isotopic composition of Pb in the peat from GL is inherently more complicated than the DK core, as Pb is derived from both atmospheric and non-atmospheric (aquatic + terrestrial) sources. Starting again in the basal peat layer, the residual fraction was found to be significantly more radiogenic than the leachable fraction (Fig. 6b). The residual fraction must reflect the isotopic composition of Pb-bearing minerals in the local rocks, and the sediments which are derived from them. In contrast, the leachable fraction of the peat must also include Pb supplied by atmospheric soil dust. Assuming that the residual fraction ($^{206}Pb/^{207}Pb = 1.3$) reflects the composition of local sediments, and that atmospheric soil dust is similar to that found in crustal rocks ($^{206}Pb/^{207}Pb =$ ca. 1.2), a mixture of 65% of the former and 35% of the latter would account for the isotopic composition of Pb in the leachable fraction ($^{206}Pb/^{207}Pb = 1.265$ for the leachate fraction of the GL sample from 88cm+ as shown Table 3).

5. SUMMARY AND CONCLUSIONS

The similar chronology of changing Hg concentrations in the surface peat layers at GL and DK (Fig. 2) suggest that *minerotrophic* peatlands also may preserve a record of *atmospheric* Hg accumulation. Using the bomb pulse curve to accurately date the past 50 yr of peat accumulation using ^{14}C, the GL peat profile provides a reconstruction of atmospheric Hg which is consistent with the 40 yr record provided by Greenland snow (Boutron et al., 1998), and complements the records provided for this region by marine (Asmund and Nielsen, 2000) and lake sediments (Landers et al., 1998; Bindler et al., 2001). Mercury fluxes in GL peats dating from preindustrial times were as low as 0.3 to 0.5 $\mu g/m^2/yr$ between AD 550 and 975 which provides an estimate of the "background" atmospheric Hg fluxes. The accumulation rate reached a maximum of 164 $\mu g/m^2/yr$ in AD 1953. The GL core indicates that the Hg flux has since declined but the value in 1995 (14 $\mu g/m^2/yr$) is clearly elevated with respect to the natural range.

The chronology of Hg accumulation rates recorded by the ombrotrophic peat bog in DK are similar to GL. The sample containing the greatest Hg accumulation rate is also the sample which is most enriched in anthropogenic Pb and As. The synchroneity of these enrichments suggests that the predominant source of all three elements was coal-burning, a view which is supported by the Pb isotope data. Moreover, the Pb isotope data show very clearly that the supply of anthropogenic Pb to the air went into decline well before the phase-out of unleaded gasoline.

The ratio of modern/pre-Industrial Hg concentrations *between* the two sites (59× in DK versus 15× in GL) is only a factor of four, compared to the differences between Pb and As EF (approximately 60 to 80 ×). The similar rates of atmospheric Hg accumulation in southern Greenland and Denmark show that atmospheric dispersion of Hg released by human activities is fundamentally different to that of As and Pb: Hg is primarily transported as Hg° in the gas phase with a residence time of one to two years, whereas Pb and and As are transported mainly as aerosols with a residence time of ca. one week (Hutchinson and Meema, 1987); this supports the prediction (Morel et al., 1998) that the *chronology* of atmospheric Hg contamination in rural and remote areas should be largely comparable because of long range, vapour phase transport of Hg.

Associate editor: M. Novak

REFERENCES

Aaby B. and Jacobsen J. (1979) Changes in biotic conditions and metal deposition in the last millenium as reflected in ombrotrophic peat in Draved Mose, Denmark. *Danm. geol. Unders., Årbog.* **1978,** 5–43.

AMAP (1998) AMAP Assessment Report: Arctic Pollution Issues. Arctic Monitoring and Assessment Programme (AMAP), Oslo, Norway, xii + 859 pp.

Andersen T. (1997) Age and petrogenesis of the Qassiarsuk carbonatite-alkaline silicate volcanic complex in the Gardar rift, South Greenland. *Mineralogical Magazine* **61,** 499–513.

Armour-Brown A., Steenfelt A., and Kunzendorf H. (1983) Uranium districts defined by reconnaissance geochemistry in South Greenland. *Journal of Geochemical Exploration* **19**, 127–45.

Asbirk S., Bertelsen U., Engelbøøl S. E., and Lorenzen H. P. (1973) En naturhistorisk undersøgelse af høøjmoserne Holmegaards Mose, Storelung og Skidendam. -Meddelelser om danske naturlokaliteter nr. 6 (Udgivet af foreningne Natur og Ungdom), København, 122 s.

Asmund G. and Nielsen S. P. (2000) Mercury in dated Greenland marine sediments. *Science of the Total Environment* **245**, 61–72.

Benoit J. M., Fitzgerald W. F., and Damman A. W. H. (1998) The biogeochemistry of an ombrotrophic bog: Evaluation of use as an archive of atmospheric mercury deposition. *Environmental Research, Section A* **78**, 118–133.

Biester H., Kilian R., Hertel C., Woda C., Mangini A., and Schöler H. F. (2002) Elevated mercury concentrations in peat bogs of South Patagonia, Chile –An anthropogenic signal. *Earth and Planetary Science Letters* **201**, 609–620.

Biester H., Martinez-Cortizas A., Birkenstock S., and Kilian R. (2003) Historic mercury records in peat bogs. The role of peat decomposition, and mass losses. *Environmental Science and Technology* **37**, 32–39.

Bindler R. (2003) Estimating the natural background atmospheric deposition rate of mercury utilizing ombrotrophic bogs in south Sweden. *Environmental Science and Technology* **37**, 40–46.

Bindler R., Renberg I., Appleby P. G., Anderson N. J., and Rose N. L. (2001) Mercury accumulation rates and spatial patterns in lake sediments from West Greenland: A coast to ice margin transect. *Environmental Science and Technology* **35**, 1736–1741.

Bollhöfer A. and Rosman K. J. R. (2001) Isotopic signatures for atmospheric lead: The Northern Hemisphere. *Geochim. Cosmochim. Acta* **65**, 1727–1740.

Bouska V. (1981) The Geochemistry of Coal. Elsevier, Amsterdam.

Boutron C. F., Vandal. V. M., Fitzgerald W. F., and Ferrari C. P. (1998) A forty year record of mercury in central Greenland snow. *Geophyical Research Letters* **25**, 3315–3318.

Boyarkina A. P., Vasil'ev N. V., Glukhov G. G., Rezchikov V. I., and Tyulyupo E. B. (1980) Gold and mercury levels in *Sphagnum* peats. *Byull. Pochv. Inst. im. V. V. Dokuchaeva.* **24**, 24–5.

Braune B., Muir D., DeMarch B., Gamberg M., Poole K., Currie R., Dodd M., Duschenko W., Eamer J., Elkin B., Evans M., Grundy S., Hebert C., Johnstone R., Kidd K., Koenig B., Lockhart L., Marshall H., Reimer K., Sanderson J., and Shutt L. (1999) Spatial and temporal trends of contaminants in Canadian Arctic freshwater and terrestrial ecosystems: a review. *Science of the Total Environment* **230**, 145–207.

Bränvall M. L., Bindler R., Emteryd O., Nilsson M., and Renberg I. (1997) Stable isotope and concentration records of atmospheric lead pollution in peat and lake sediments in Sweden. *Water Air Soil Pollution* **100**, 243–252.

Christensen J. H., Goodsite M. E., Heidam N. Z., Skov H., and Wåhlin P. (2002) Atmospheric Environment. Chap. 1. In *AMAP Greenland Environment (1997–2001)* (eds. F. Riget, J. Christensen, and P. Johansen). Ministry of Environment, Denmark Department of Atmospheric Environment, National Environmental Research Institute of Denmark, Roskilde, Denmark.

Clymo R. S. (1987) The ecology of peatlands. *Science Progress (Oxford)* **71**, 593–614.

Cocozza C., D'Orazio D., Miano T. M., and Shotyk W. (2003) Characterization of solid and aqueous phases of a peat bog profile using molecular fluorescence spectroscopy, ESR, and FT–IR. *Org. Geochem.* **34**:49–60.

Emmanuel S. and Erel Y. (2002) Implications from concentrations and isotopic data for Pb partitioning processes in soils. *Geochim. Cosmochim. Acta* **66**, 2517–2527.

Farmer J. G., Mackenzie A. B., Sugden C. L., Edgar P. J., and Eades L. J. (1997) A comparison of the historical lead pollution records in peat and freshwaer lake sediments from central Scotland. *Water Air Soil Pollution* **100**, 253–270.

Farmer J. G., Eades L. J., and Graham M. C. (1999) The lead content and isotopic composition of Br. coals and their implications for past and present releases of lead to the U.K. environment. *Environmental Geochemistry and Health* **21**, 257–272.

Flament P., Bertho M.-L., Deboudt K., Veron A., and Puskaric E. (2002) European isotopic signatures for lead in atmospheric aero-

sols: a source apportionment based upon ^{206}Pb/^{207}Pb ratios. *Science of the Total Environment* **296**, 35–57.

Fitzgerald W. F. and Clarkson T. W. (1991) Mercury and methylmercury: Present and future concerns. *Environmental Health Perspectives* **96**, 159–166.

Fitzgerald W. F., Engstrom D. R., Mason R. P., and Nater E. A. (1997) The case for atmospheric mercury contamination in remote areas. *Environmental Science and Technology* **32**, 1–7.

Frei R., Villa I. M., Nägler T. F., Kramers J. D., Przybylowicz W. J., Prozesky V. M., Hofmann B. A., and Kamber B. S. (1997) Single mineral dating by the Pb-Pb step-leaching method, assessing the mechanism. *Geochim. Cosmochim. Acta* **61**, 393–414.

Gobeil C., Macdonald R. W., and Smith J. N. (1999) Mercury profiles in sediments of the Arctic Ocean basins. *Environmental Science and Technology* **33**, 4194–4198.

Goodsite M. E. (2000) Heavy metal deposition determined by correlation with 14C. M.Sc. thesis, University of Southern Denmark.

Goodsite M. E., Heinemeier J., Rom W., Lange T., Ooi S., Appleby, P. G., Shotyk W., van der Knaap W. O., Lohse C., and Hansen T. S. (2002) High resolution AMS ^{14}C dating of post bomb peat archives of atmospheric pollutants. *Radiocarbon* **43** *(2B)*, 495–515.

Hagner C. (2000) European regulations to reduce lead emissions from automobiles - did they have an economic impact on the German gasoline and automobile markets? *Regional Environmental Change* **1**, 135–151.

Harlavan Y. and Erel Y. (2002) The release of Pb and REE from granitoids by the dissolution of accessory phases. *Geochim. Cosmochim. Acta* **66**, 837–848.

Hutchinson T. C. and Meema K. M. eds. 1987 *Lead, Mercury, Cadmium, and Arsenic in the Environment.* SCOPE 31, John Wiley and Sons, New York.

Jensen A. and Jensen A. (1991) Historical rates of mercury in Scandinavia estimated by dating and measurement of mercury in cores of peat bogs. *Water, Air and Soil Pollution* **56**, 769–777.

Jensen F. P. and Fenger J. (1994) The air quality in Danish urban areas. *Environmental Health Perspectives* **102**, 55–60.

Kempter H. and Frenzel B. (1999) The local nature of anthropogenic emission sources on the elemental content of nearby ombrotrophic peat bogs, Vulkaneifel, Germany. *Science of the Total Environment* **241**, 117–128.

Kempter H. and Frenzel B. (2000) The impact of early mining and smelting on the local tropospheric aerosol detected in ombrotrophic peat bogs in the Harz, Germany. *Water Air, Soil Pollution* **121**, 93–108.

Kempter H., Görres M., and Frenzel B. (1997) Ti and Pb concentrations in rainwater-fed bogs in Europe as indicators of past anthropogenic activities. *Water Air Soil Pollution* **100**, 367–377.

Kober B., Wessels M., Bollhöfer A., and Mangini A. (1999) Pb isotopes in sediments of Lake Constance, Central Europe constrain the heavy metal pathways and the pollution history of the catchment, the lake and the regional atmosphere. *Geochim. Cosmochim. Acta* **63**, 1293–1303.

Kramers J. D. and Tolstikhin I. D. (1997) Two terrestrial lead isotope paradoxes, forward transport modelling, core formation, and the history of the continental crust. *Chem. Geol.* **139**, 75–110.

Lamborg C. H., Fitzgerald W. F., O'Donnell J., and Torgersen T. (2002) A non-steady state compartmental model of global-scale mercury biogeochemistry with interhemispheric atmospheric gradients. *Geochim. Cosmochim. Acta* **66**, 1105–1118.

Landers D. H., Gubala C., Verta M., Lucotte M., Johansson K., Vlasova T., and Lockhart W. L. (1998) Using lake sediment mercury flux ratios to evalute the regional and continental dimensions of mercury deposition in Arctic and Boreal ecosystems. *Atmospheric Environment* **32**, 919–928.

Lin C-J. and Pehkonen S. O. (1999) The chemistry of atmospheric mercury: A review. *Atmospheric Environment* **33**, 2067–2079.

Lindberg S., Stokes P. M., Goldberg E., and Wren C. (1987) Group report: Mercury. In *Lead, Mercury, Cadmium, and Arsenic in the Environment* (eds. T.C. Hutchinson and K.M. Meema) pp. 17–33. John Wiley and Sons, New York.

Lodenius M., Seppänen A., and Uusi-Rauva A. (1983) Sorption and mobilization of mercury in peat soil. *Chemosphere* **12**, 1575–1581.

Martinez-Cortizas A., Pontevedra Pomba X., Novoa Munoz J. C., and Garcia-Rodeja E. (1997) Four thousand years of atmospheric Pb, Cd,

and Zn deposition recorded by the ombrotrophic peat bog of Penido Vello (northwestern Spain). *Water Air Soil Pollution* **100**, 387–403.

Martinez-Cortizas A. M., Ponteedra Pomba X., Garcia-Rodeja E., Novoa Munoz J. C., and Shotyk W. (1999) Mercury in a Spanish peat bog: Archive of climate change and atmospheric metal deposition. *Science* **284**, 939–942.

MacKenzie A. B., Farmer J. G., and Sugden C. L. (1997) Isotopic evidence of the relative retention and mobility of lead and radiocaesium in Scottish ombrotrophic peats. *Science of the Total Environment* **203**, 115–127.

MacKenzie A. B., Logan E. M., Cook G. T., and Pulford I. D. (1998) Distributions, inventories, and isotopic composition of lead in ^{210}Pb-dated peat cores from contrasting biogeochemical environments: Implications for lead mobility. *Science of the Total Environment* **223**, 25–35.

Monna F., Lancelot J., Croudace I. W., Cundy A. B., and Lewis J. T. (1997) Pb isotopic composition of airborne particulate material from France and the southern United Kingdom: Implications for Pb pollution sources in urban areas. *Environmental Science and Technology* **31**, 2277–2286.

Morel F. M. M., Kraepiel A. M. L., and Amyot M. (1998) The cycle and bioaccumulation of mercury. *Ann. Reviews of Ecological Systems* **29**, 543–566.

Naucke W., Heathwaite A. L., Eggelsmann R., and Schuch M. (1993) Mire chemistry. In *Mires. Process, Exploitation, and Conservation* (eds. K. Göttlich; trans. J. Cooke). John Wiley and Sons, New York.

Norton S. A., Evans G. C., and Kahl J. S. (1997) Comparison of Hg and Pb fluxes to hummocks and hollows of ombrotrophic Big Heath Bog and to nearby Sargent Mt. Pond, Maine, USA. *Water Air Soil Pollution* **100**, 271–286.

Novak M., Emmanuel S., Vile M. A., Erel Y., Veron A., Paces T., Wieder R. K., Vanecek M., Stepanova M., Brizova E., and Hovorka J. (2003) Origin of lead in eight Central European Peat Bogs determined from isotope ratios, strengths and operation times of regional pollution sources. *Environmental Science and Technology* **37**, 437–445.

Oechsle D. (1982) Untersuchungen zur Mobilität von Quecksilber-Spezies in Hochmooren und Möglichkeiten zu ihrer analytische Trennung und Bestimmung. Ph.D.Thesis, Universität Stuttgart.

Pheiffer-Madsen P. (1981) Peat bog records of atmospheric mercury deposition. *Nature* **293**, 127–129.

Puxbaum H. (1991) Metal compounds in the atmosphere. In *Metals and their Compounds in the Environment* (ed. E. Merian) pp. 257–286, VCH, Weinheim.

Rasmussen P. E. (1994) Current methods of estimating atmospheric mercury fluxes in remote areas. *Environmental Science and Technology* **28**, 2233–2241.

Reuer M. K. and Weiss D. J. (2002) Anthropogenic lead dynamics in the terrestrial and marine environment. *Philosophical Transactions of the Royal Society of London A* **360**, 2889–2904.

Roos-Barraclough F. and Shotyk W. (2003) Millennial-scale records of atmospheric mercury deposition obtained from ombrotrophic and minerotrophic peat from the Swiss Jura Mountains. *Environmental Science and Technology* **37** (2), 235–244.

Roos-Barraclough F., Martinez-Cortizas A., Garcia-Rodeja E., and Shotyk W. (2002a) A 14,500 year record of the accumulation of atmospheric mercury in peat: volcanic signals, anthropogenic influences, and a correlation to bromine accumulation. *Earth Planet. Sci. Lett.* **202** (2), 435–451.

Roos-Barraclough F., Biester H. F., Goodsite M. E., Martinez-Cortizas A., and Shotyk W. (2002b) Analytical protocol for measuring total Hg concentrations in peat cores. *Science of the Total Environment* **292**, 129–139.

Rosman K. J. R., Chisholm W., Boutron C. F., Candelone J. P., Jaffrezo J.-L., and Davidson C. I. (1998) Seasonal variations in the origin on lead in snow at Dye 3, Greenland. *EPSL* **160**, 383–389.

Salvato N. and Pirola C. (1996) Analysis of mercury traces by means of solid sample atomic absorption spectrometry. *Mikrochimica Acta* **123**, 63–71.

Schaller M., Steiner O., Studer I., Frei R., and Kramers J. D. (1997) Pb stepwise leaching (PbSL) dating of garnet - addressing the inclusion problem. *Schweizerische Mineralogische Petrographische Mitteilungen* **77**, 113–121.

Schroeder W. H. and Munthe J. (1998) Atmospheric mercury - an overview. *Atmospheric Environment* **32**, 809–822.

Shotyk W. (1988) Review of the inorganic geochemistry of peats and peatland waters. *Earth-Science Reviews* **25** (2), 95–176.

Shotyk W. (2002) The chronology of anthropogenic, atmospheric Pb deposition recorded by peat cores in 3 minerotrophic peat deposits from Switzerland. *Science of the Total Environment* **292**, 19–31.

Shotyk W., Blaser P., Grünig A., and Cheburkin A. K. (2000) A new approach for quantifying cumulative, anthropogenic, atmospheric lead deposition using peat cores from bogs: Pb in eight Swiss peat bog profiles. *Science of the Total Environment* **249**, 257–280.

Shotyk W., Cheburkin A. K., Appleby P. G., Fankhauser A., and Kramers J. D. (1997) Lead in three peat bog profiles, Jura Mountains, Switzerland: enrichment factors, isotopic composition, and chronology of atmospheric deposition. *Water Air and Soil Pollution* **100** (3/4), 297–310.

Shotyk W., Cheburkin A. K., Appleby P. G., Fankhauser A., and Kramers J. D. (1996) Two thousand years of atmospheric arsenic, antimony, and lead deposition recorded in a peat bog profile, Jura Mountains, Switzerland. *Earth Planet. Sci. Lett.* **145**, E1–E7.

Shotyk W., Krachler M., Martinez-Cortizas A., Cheburkin A. K., Emons H. (2002a) A peat bog record of natural, pre-anthropogenic enrichments of trace elements in atmospheric aerosols since 12,370 14C yr BP, and their variation with Holocene climate change. *Earth and Planet. Sci. Lett.* 21–37.

Shotyk W., Nesbitt H. W., and Fyfe W. S. (1992) Natural and anthropogenic enrichments of trace metals in peat profiles. *International Journal of Coal Geology* **20**, 49–84.

Shotyk W., Weiss D., Appleby P. G., Cheburkin A. K., Frei R., Gloor M., Kramers J. D., Reese S., and van der Knaap W. O. (1998) History of atmospheric lead deposition since 12,370 ^{14}C yr BP recorded in a peat bog profile, Jura Mountains, Switzerland. *Science* **281**, 1635–1640.

Shotyk W., Weiss D., Heisterkamp M., Cheburkin A. K., and Adams F. C. (2002b) A new peat bog record of atmospheric lead pollution in Switzerland: Pb concentrations, enrichment factors, isotopic composition, and organolead species. *Environ. Sci. Technol.* **36**, 3893–3900.

Shotyk W., Weiss D., Heisterkamp M., Cheburkin A. K., and Adams F. C. (2003) A new peat bog record of atmospheric lead pollution in Switzerland: Pb concentrations, enrichment factors, isotopic composition, and organolead species. *Environmental Science and Technology* **37** (2), 235–244.

Shotyk W., Weiss D., Kramers J. D., Frei R., Cheburkin A. K., Gloor M., and Reese S. (2001) Geochemistry of the peat bog at Etang de la Gruère, Jura Mountains, Switzerland, and its record of atmospheric Pb and lithogenic trace elements (Sc, Ti, Y, Zr, Hf and REE) since 12,370 ^{14}C yr BP. *Geochim. Cosmochim. Acta* **65** (14), 2337–2360.

Steinmann P. and Shotyk W. (1997) The pH, redox chemistry, and speciation of Fe and S in pore waters from two contrasting *Sphagnum* bogs, Jura Mountains, Switzerland. *Geochim. Cosmochim. Acta* **61** (6), 1143–1163.

Swaine D. J. (1990) *Trace Elements in Coal.* Butterworth, London.

Todt W., Cliff R. A., Hanser A., and Hofmann A. W. (1993) Recalibration of NBS lead standards using a ^{202}Pb+ ^{205}Pb double spike. *Terra Abstracts* **5(Suppl. 1)**, 396.

Valkovic V. (1983) *Trace Elements in Coal.* 2 vols. CRC Press, Boca Raton.

Vile M. A., Novak M. J., Brizova E., Wieder R. K., and Schell W. R. (1995) Historical rates of atmospheric Pb deposition using ^{210}Pb dated peat cores: Corroboration, computation, and interpretation. *Water, Air, Soil Pollution* **79**, 89–106.

Vile M. A., Wieder R. K., and Novak M. (1999) Mobility of Pb in *Sphagnum*-derived peat. *Biogeochemistry* **45**, 35–52.

Wardenaar E. C. P. (1987) A new hand tool for cutting peat profiles. *Canadian Journal of Botany* **65**, 1772–1773.

Wedepohl K. H. (1995) The composition of the continental crust. *Geochim. Cosmochim. Acta* **59**, 1217–1232.

Weiss D., Shotyk W., Appleby P. G., Cheburkin A. K., and Kramers J. D. (1999a) Atmospheric Pb deposition since the Industrial Revolution recorded by five Swiss peat profiles: Enrichment factors, fluxes, isotopic compositon, and sources. *Environmental Science and Technology* **33**, 1340–1352.

Weiss D., Shotyk W., Gloor M., and Kramers J. D. (1999b) Herbarium specimens of *Sphagnum* moss as archives of recent and past atmospheric Pb deposition in Switzerland: Isotopic composition and source assessment. *Atmospheric Environment* **33**, 3751–3763.